

# Non-peptidic Inhibitors of Human Leukocyte Elastase. 4. Design, Synthesis, and *in Vitro* and *in Vivo* Activity of a Series of $\beta$ -Carbolinone-Containing Trifluoromethyl Ketones

Chris A. Veale,<sup>\*,†</sup> James R. Damewood, Jr.,<sup>\*,‡</sup> Gary B. Steelman,<sup>†</sup> Craig Bryant,<sup>†</sup> Bruce Gomes,<sup>§</sup> and Joseph Williams<sup>§</sup>

Departments of Medicinal Chemistry and Pharmacology, ZENECA Pharmaceuticals, A Business Unit of ZENECA Inc., Wilmington, Delaware 19897

Received August 3, 1994<sup>⊗</sup>

A novel series of human leukocyte elastase (HLE) inhibitors containing the  $\beta$ -carbolinone ring system are reported. The design of these trifluoromethyl ketone-based inhibitors used a combination of structural information obtained from X-ray crystallography and molecular modeling investigations. The  $\beta$ -carbolinone ring in these compounds serves as a highly efficient peptidomimetic for the P<sub>2</sub>–P<sub>3</sub> region of peptidyl trifluoromethyl ketone inhibitors of HLE. Several of the  $\beta$ -carbolinones exhibit significant *in vitro* potency, with K<sub>i</sub> values in the nanomolar range. Using aqueous molecular dynamics simulations, realistic models for the molecular recognition of these inhibitors by HLE have been obtained and are discussed. This series of compounds are found to have excellent selectivity for HLE over a number of other proteolytic enzymes, including closely related enzymes such as porcine pancreatic elastase.

## Introduction

Human leukocyte elastase (HLE) is one of several serine proteases contained in the azurophilic granules of polymorphonuclear leukocytes. The physiological role of this enzyme is largely thought to be intracellular, taking part in phagocytosis and host defense.<sup>1</sup> When present in the extracellular environment, the ability of elastase to degrade structural proteins found in connective tissues (e.g., elastin and type IV collagen) has led to speculation that the enzyme aids in the migration of neutrophils into the airways in response to chemotatic factors.<sup>2–4</sup> HLE has been shown to be an extremely potent mucus secretagogue.<sup>5</sup> The effect of elastase on mucus secretion is thought to be due to the proteolytic activity of the enzyme as it is blocked by active site-directed inhibitors such as ICI-200,355 (1, Figure 1).<sup>6</sup>

Extracellular elastase activity is tightly controlled in the pulmonary system by a number of proteinaceous inhibitors.  $\alpha_1$ -Protease inhibitor ( $\alpha_1$ PI) is thought to be primarily responsible for protection of the lower airways from elastolytic damage, while secretory leukocyte protease inhibitor appears to shield the upper airways.<sup>7,8</sup> In a number of pulmonary pathophysiological states, these proteins ineffectively regulate HLE activity. The resulting unconstrained elastolytic activity is associated with the abnormal tissue turnover found in pulmonary emphysema<sup>9</sup> and in diseases such as cystic fibrosis and chronic bronchitis in which mucus hypersecretion and impaired host defense are major components.<sup>10–12</sup>

There continues to be considerable interest in the development of synthetic inhibitors of HLE to be used as therapy in disease states in which elastase activity is ineffectively controlled by endogenous inhibitors.<sup>13–15</sup> Previous reports from these laboratories have disclosed several different series of reversible, peptidic inhibitors of HLE (see Figure 1). These inhibitors demonstrate

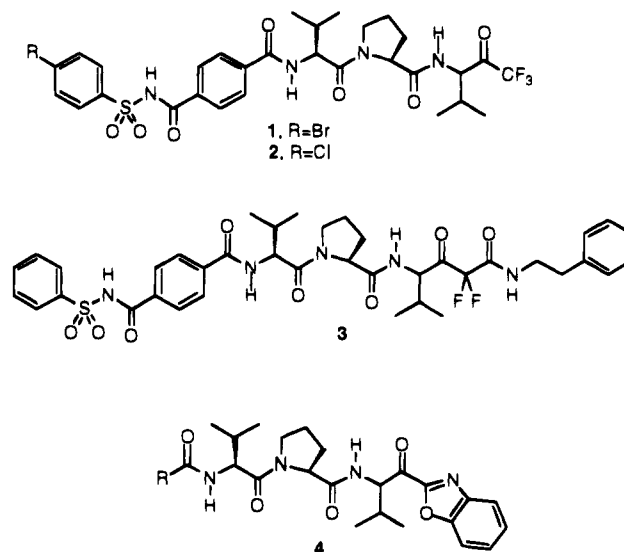


**Figure 1.** Peptidic HLE inhibitors: 1, ICI-200,355; 2, ICI-200,880; 3, difluoroketone inhibitor; 4,  $\alpha$ -ketobenzoxazole inhibitor.

potent, long-lasting inhibition of elastase activity after intratracheal administration in animal models.<sup>16,17</sup> One of these compounds (ICI-200,880, 2) has undergone extensive clinical evaluation.<sup>18</sup> As a follow-up to ICI-200,880, we sought to develop an HLE inhibitor that could be administered by the oral route (po). The lack of oral activity found in compounds 1–4 (Figure 1), coupled with the knowledge that peptidic compounds can suffer from poor oral bioavailability, suggested that we should attempt to replace peptidic portions of these inhibitors with appropriate mimetics. A key step in this process was the discovery that the P<sub>3</sub>–P<sub>2</sub>, Val-Pro unit in 1–4 could be replaced by a functionalized pyridone ring (e.g., 5, Figure 2), providing potent inhibitors of HLE.<sup>19,20</sup> We now report the extension of this work to a series of tricyclic  $\beta$ -carbolinones (e.g., 6, Figure 2). These compounds are also found to be potent inhibitors of HLE.

<sup>†</sup> Pulmonary Chemistry Section.

<sup>‡</sup> Structural Chemistry Section.

<sup>§</sup> Department of Pharmacology.

<sup>⊗</sup> Abstract published in *Advance ACS Abstracts*, December 15, 1994.

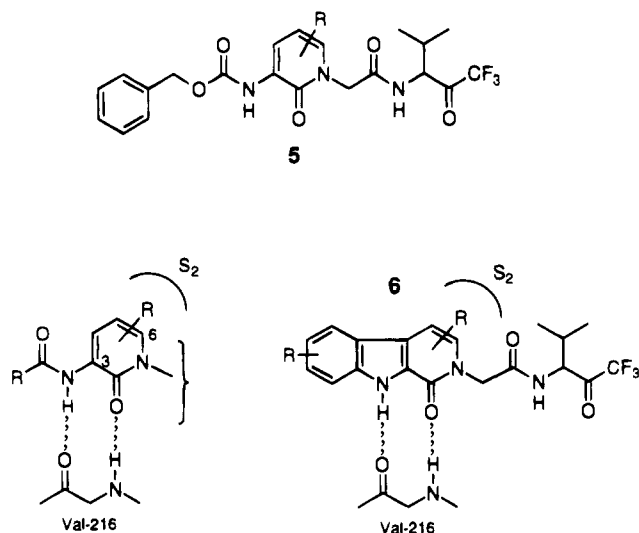


**Figure 2.** Top: General structure for pyridone-based trifluoromethyl ketone inhibitors of HLE (**5**). Bottom left: Partial representation of binding mode of pyridone-based inhibitors with HLE. Bottom right: General structure for  $\beta$ -carbolinone-based trifluoromethyl ketone inhibitors of HLE (**6**) and partial representation of their binding mode with HLE.

### Initial Design Considerations

Our design efforts were greatly aided by the availability of several crystal structures of peptidic inhibitors complexed to either HLE or the closely related enzyme porcine pancreatic elastase (PPE).<sup>21–24</sup> The X-ray crystal structure of the complex formed between HLE and the third domain of the turkey ovomucoid inhibitor (TOMI)<sup>24</sup> revealed a number of interesting enzyme–inhibitor interactions (Figure 3a). In this structure, a portion of the Leu 18I side chain of TOMI occupies the  $S_1$  specificity pocket of HLE, consistent with the preference of the enzyme for small hydrophobic residues at this site. In addition, several hydrogen-bonding interactions are formed between the inhibitor and enzyme. Particularly noteworthy are the  $\beta$ -sheet, reciprocal pair of hydrogen bonds formed between Val 216 (HLE) and the P3 residue, Cys 16I (TOMI). The crystal structure of the HLE complex with the *irreversible* inhibitor MeOSuc-Ala-Ala-Pro-Val-CH<sub>2</sub>Cl<sup>25</sup> also displays this reciprocal pair of hydrogen bonds in the  $\beta$ -sheet region (Figure 3b). While outside the range typically observed for hydrogen bonding interactions, both TOMI and MeOSuc-Ala-Ala-Pro-Val-CH<sub>2</sub>Cl direct carbonyl oxygens (from Pro 14I (3.7 Å) and Suc (3.5 Å), respectively) toward the NH of Gly 218. Previously reported simulations of a *p*-CH<sub>3</sub>CONHC<sub>6</sub>H<sub>4</sub>SO<sub>2</sub>-substituted pyridone revealed that a hydrogen-bonding interaction can form between this NH of HLE and an appropriately substituted inhibitor.<sup>19d</sup>

The X-ray crystal structure of a peptidic trifluoromethyl ketone (TFMK) inhibitor, acetyl-Ala-Pro-Val-TFMK,<sup>21</sup> covalently bound to PPE shows similar binding interactions (Figure 3c) to those observed in the HLE structures, including the reciprocal pair of hydrogen bonds in the P3 region. This inhibitor places the Val side chain in the  $S_1$  pocket and forms two hydrogen bonds between the trifluoromethyl oxyanion and the NH atoms of Ser 195 and Gly 193. While similar in these aspects, interesting differences have also been noted for the PPE and HLE binding environments.<sup>26</sup>

A major simplification of the peptidic inhibitors was realized from inspection of their orientation in the  $P_3$  region when bound to HLE. The near coplanar arrangement of the  $\beta$ -sheet hydrogen-bonding moieties suggested that their incorporation into an appropriate heterocycle would maintain critical interactions while eliminating two stereogenic centers. The aminopyridone series (e.g., **5**, Figure 2) demonstrated the validity of this hypothesis. A natural extension of this effort involved the incorporation of the NH donor of **5** into a cyclic system, thus opening the possibility of new classes of polycyclic compounds that could serve as potential HLE inhibitors. Of the many possible polycyclic ring systems that present the needed H-bond donor–acceptor pair, we chose to explore a series of  $\beta$ -carbolinones (e.g., **6**, Figure 2). This decision was motivated both by the ease of synthesis of this ring system and the expectation that the  $\beta$ -carbolinone nucleus would be easily amenable to further functionalization.

### Chemistry

The intermediates and compounds described in Table 1 were prepared as shown in Scheme 1–4. Compounds in the tetrahydro- $\beta$ -carbolinone series were prepared by general method A, described in Scheme 1. The substituted 1,2,3,4-tetrahydro-1-oxo- $\beta$ -carbolines **7** used as starting materials were obtained commercially or prepared by literature methods.<sup>27</sup> Selective protection of the more acidic 9-position NH was achieved by formation of the monoanion with sodium hydride followed by alkylation to afford the SEM-protected compound **8**. A second deprotonation and subsequent alkylation using iodide **10**<sup>28</sup> gave compound **11**. Removal of the SEM and *tert*-butyldimethylsilyl protecting groups using fluoride ion followed by oxidation of the trifluoromethyl alcohol using a modified Pfitzner–Moffatt procedure provided the desired trifluoromethyl ketones **12a–d**. Oxidation of the tricyclic ring system using DDQ yielded dihydro- $\beta$ -carbolinones **13a–f**. This general method worked well for the preparation of compounds with substitution in the 6-, 7-, and 8-positions of the  $\beta$ -carbolinone nucleus. However, it was not useful for the preparation of 3-substituted  $\beta$ -carbolinones. Instead, a different method of synthesis of the dihydro- $\beta$ -carbolinone ring system was employed (general method B, Scheme 2) where the tricyclic ring system is formed by the acid-catalyzed ring closure of an acetal (**15**). In this strategy it is important that a latent form ( $R_3$  in Scheme 2) of what will become the trifluoromethyl ketone-containing side chain be incorporated prior to cyclization, as attempts to incorporate this side chain by alkylation procedures similar to those used in Scheme 1 provide only O-alkylated products. Protection of the indole nitrogen in **15** is not required to control the regiochemical course of the cyclization (e.g., C- vs N-alkylation); however higher yields of cyclized product **16** are obtained when the nitrogen is protected, and thus the *N*-benzyl protecting group was routinely employed in our syntheses. Transformation of **16** into the requisite acid **17** was achieved by an oxidative three-step sequence or basic hydrolysis. An EDC-mediated coupling of the resulting acid to the amine **9**<sup>16</sup> (Scheme 1) followed by removal of the benzyl protecting group with aluminum chloride and oxidation of the alcohol to the trifluoromethyl ketone afforded compounds of the general structure **19**.

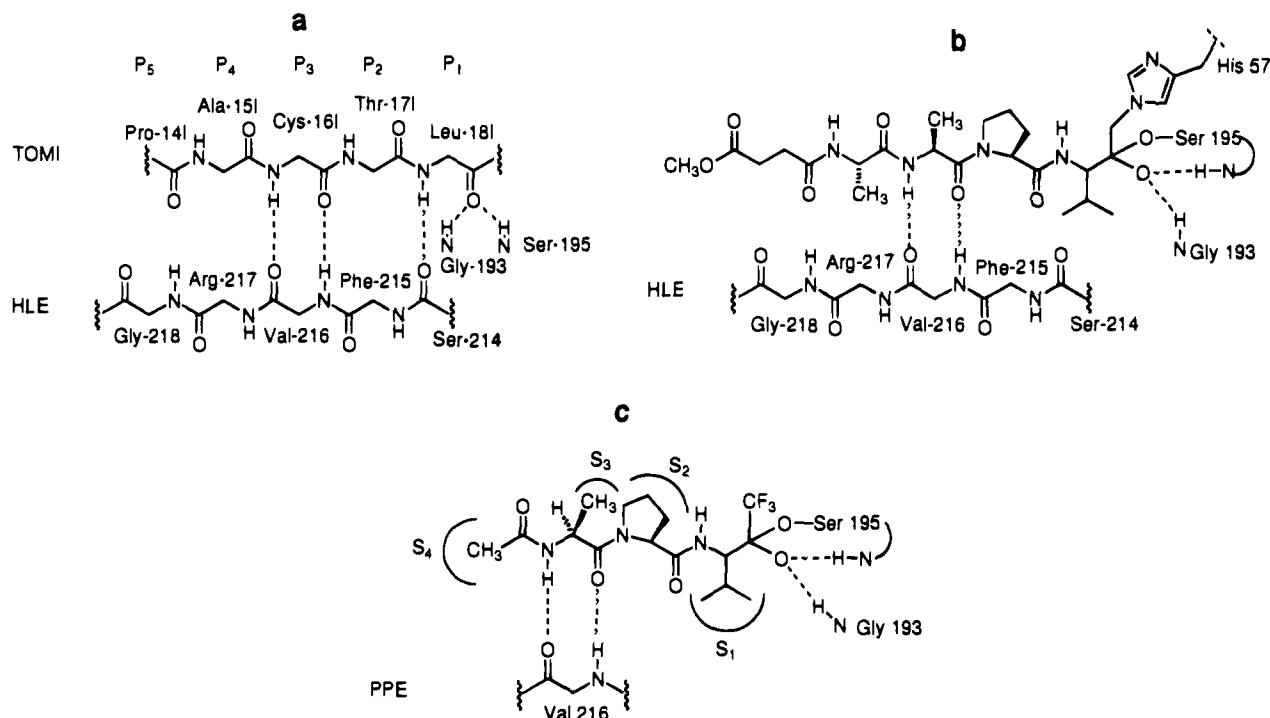
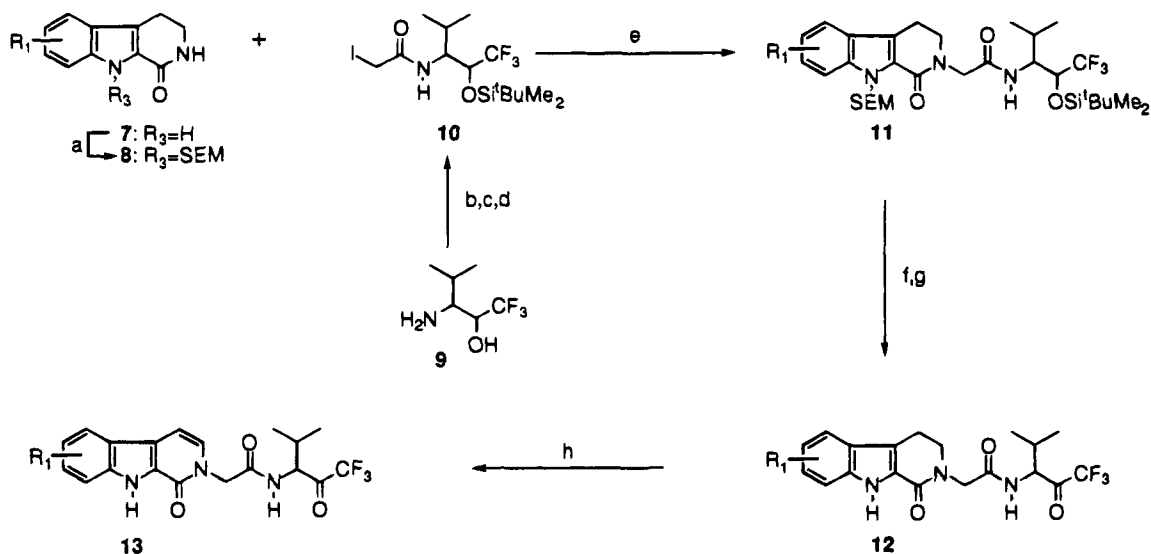


**Figure 3.** (a) Schematic representation of the hydrogen-bonding interactions in the P<sub>1</sub>–P<sub>5</sub> binding segment of TOMI with HLE (ref 24). (b) Schematic representation of interactions between MeOSuc-Ala-Ala-Pro-Val-CH<sub>2</sub>Cl and HLE (ref 25b). (c) Schematic representation of interactions between Ac-Ala-Pro-Val-TFMK and PPE (ref 21).

#### Scheme 1. General Method A<sup>a</sup>



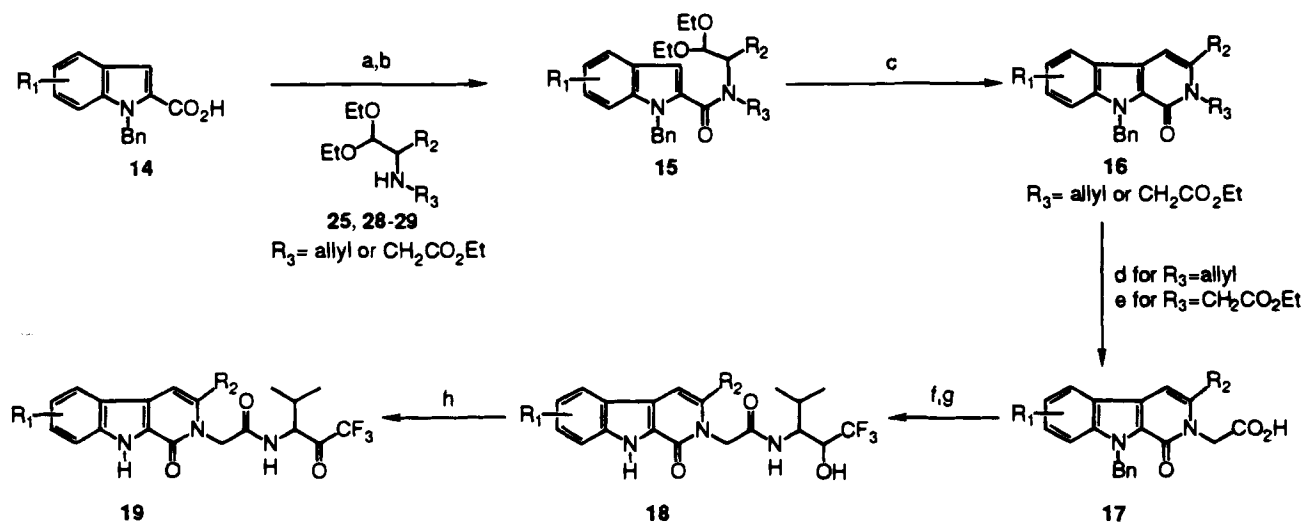
<sup>a</sup> Generic groups R<sub>1</sub> and R<sub>2</sub> are defined in Table 1. Reagents: (a) NaH, [2-(trimethylsilyl)ethoxy]methyl chloride, THF; (b) chloroacetyl chloride, 4-methylmorpholine, THF; (c) *tert*-butyldimethylsilyl triflate, 2,6-lutidine, CH<sub>2</sub>Cl<sub>2</sub>; (d) NaI, acetone; (e) NaH, THF; (f) 1 M Bu<sub>4</sub>NF in THF, reflux; (g) EDC, Cl<sub>2</sub>CHCO<sub>2</sub>H, DMSO, toluene; (h) DDQ, dioxane.

In the case of compound **19c**, difficulty in the preparation of the required 8-cyanoindole-2-carboxylic acid by conventional methods of indole ring synthesis prompted us to devise a new method, which is shown in Scheme 3. The known ketone **22**<sup>29</sup> was transformed in a one-pot sequence, via cyanohydrin formation and subsequent elimination, into the vinyl nitrile. Oxidation of the nitrile with DDQ followed by benzylation of the nitrogen and ester hydrolysis provided 8-cyanoindole-2-carboxylic acid **23**.

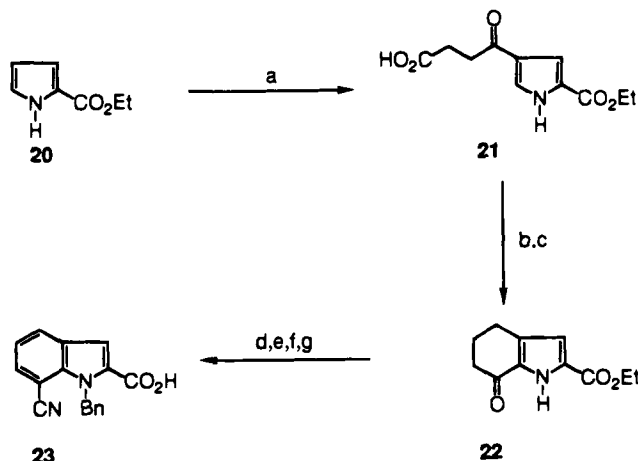
The amino acetals **25**, **28**, and **29** used in Scheme 2 were made (Scheme 4) either by a reductive amination in cases where the keto acetal was readily available

(e.g., **24**) or via alkylation of the amino acetals<sup>30</sup> (**26** and **27**) with ethyl bromoacetate.

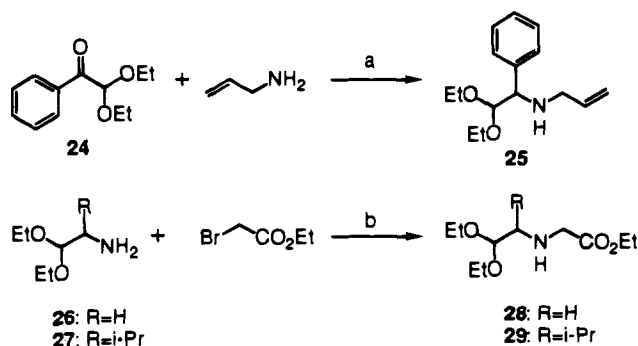
Conversion of the 8-cyano- $\beta$ -carbolinones into their aldehyde, ester, and acid derivatives **32**–**34** is detailed in Scheme 5. The nitrile functionality in **18** was selectively reduced using Raney nickel to yield the corresponding aldehyde **30**. Further transformation of **30** provided ester **33** and acid **34**. The incorporation of other polar substituents in the 8-position is shown in Scheme 6. The 8-(benzyloxy)- $\beta$ -carbolinone **17** was coupled with amine **9** to give **35**. Depending upon the severity of the hydrogenolysis conditions used, either one or both of the benzyl protecting groups could be

Scheme 2. General Method B<sup>a</sup>

<sup>a</sup> Generic groups  $R_1$  and  $R_2$  are defined in Table 1. Reagents: (a)  $(\text{COCl})_2$ ,  $\text{CH}_2\text{Cl}_2$ , DMF; (b) **25**, **28**, or **29**,  $\text{Et}_3\text{N}$ ,  $\text{CH}_2\text{Cl}_2$ ; (c)  $\text{H}_2\text{SO}_4$ , ether; (d) (i)  $\text{OsO}_4$ , *N*-methylmorpholine *N*-oxide, THF,  $\text{H}_2\text{O}$ ; (ii)  $\text{NaIO}_4$ , ethanol,  $\text{H}_2\text{O}$ ; (iii)  $\text{NaClO}_2$ , 2-methyl-2-butene,  $\text{NaH}_2\text{PO}_4$ , *tert*-butyl alcohol, THF,  $\text{H}_2\text{O}$ ; (e)  $\text{LiOH}$ , THF, MeOH,  $\text{H}_2\text{O}$ ; (f) **9**, EDC, HOBT,  $\text{Et}_3\text{N}$ , DMF; (g)  $\text{AlCl}_3$ , benzene,  $\text{CH}_3\text{NO}_2$ ; (h) EDC,  $\text{Cl}_2\text{CHCO}_2\text{H}$ , toluene, DMSO.

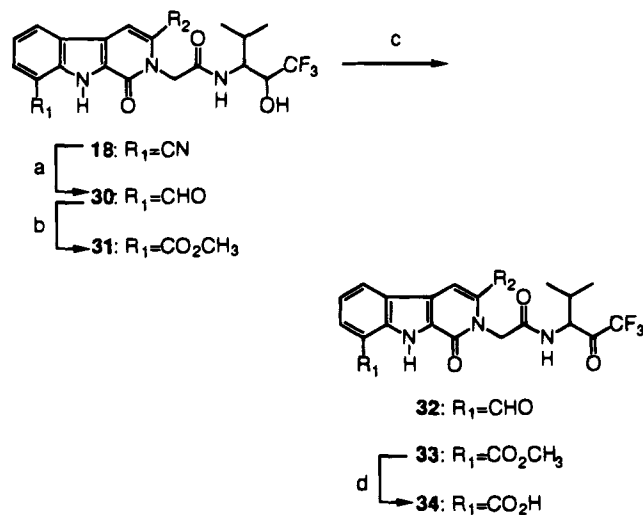
Scheme 3<sup>a</sup>

<sup>a</sup> Reagents: (a) succinic anhydride,  $\text{AlCl}_3$ ,  $\text{CH}_3\text{NO}_2$ ; (b)  $\text{H}_2$  Pd/C,  $\text{CF}_3\text{CO}_2\text{H}$ ,  $\text{CH}_3\text{CO}_2\text{H}$ , 60 °C; (c)  $(\text{CF}_3\text{CO})_2\text{O}$ ,  $\text{CF}_3\text{CO}_2\text{H}$ ; (d)  $\text{TMSCN}$ ,  $\text{ZnI}_2$ , benzene; then  $\text{POCl}_3$ , pyridine, 80 °C; (e) DDQ, dioxane; (f)  $\text{NaH}$ , benzyl bromide, DMF; (g)  $\text{LiOH}$ , THF,  $\text{CH}_3\text{OH}$ ,  $\text{H}_2\text{O}$ .

Scheme 4<sup>a</sup>

<sup>a</sup> Reagents: (a)  $\text{NaBH}_3\text{CN}$ , acetic acid, 3 Å molecular sieves, ethanol; (b)  $\text{Et}_3\text{N}$ , THF.

removed. The 8-hydroxy compound **38** was prepared by protection of the phenolic hydroxyl with *tert*-butyldimethylsilyl chloride followed by oxidation of the trifluoromethyl alcohol and removal of the silyl protecting group using fluoride ion. Alternatively, selective

Scheme 5. General Method C<sup>a</sup>

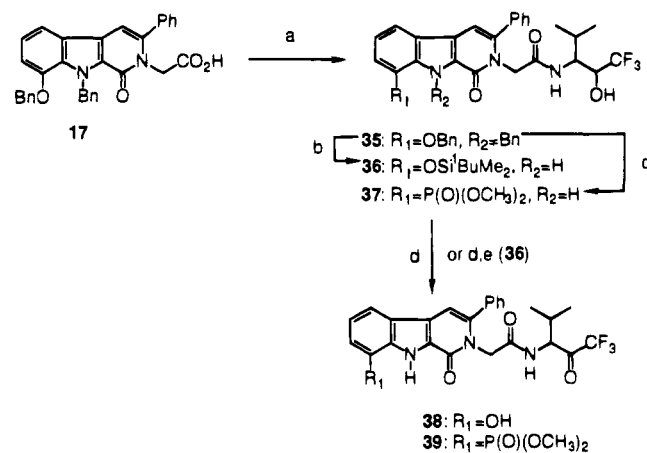
<sup>a</sup> Generic group  $R_2$  is defined in Table 1. Reagents: (a) Raney nickel,  $\text{NaH}_2\text{PO}_4 \cdot \text{H}_2\text{O}$ , pyridine, acetic acid,  $\text{H}_2\text{O}$ ; (b) (i)  $\text{NaClO}_2$ , 2-methyl-2-butene,  $\text{NaH}_2\text{PO}_4$ , *tert*-butyl alcohol, THF,  $\text{H}_2\text{O}$ ; (ii)  $\text{CH}_2\text{N}_2$ , ether; (c) EDC,  $\text{Cl}_2\text{CHCO}_2\text{H}$ , DMSO, toluene; (d)  $\text{LiOH}$ , THF,  $\text{H}_2\text{O}$ .

hydrogenolysis of the benzyloxy group in **35** followed by triflate formation, palladium-catalyzed coupling with dimethyl phosphite, and removal of the *N*-benzyl protecting group gave compound **37**. Oxidation of **37** by the previously described procedure afforded **39**. A similar sequence, but starting with 6-(benzyloxy)indole-2-carboxylic acid in Scheme 2, was used to prepare the 6-phosphonate derivative **40**.

## In Vitro HLE Inhibition

The *in vitro* activity of the compounds in Table 1 was measured by their ability to inhibit the elastase-mediated hydrolysis of the synthetic substrate MeOSuc-Ala-Ala-Pro-Val-pNA using the method described by Stein and co-workers.<sup>31</sup> cursory inspection of Table 1 reveals that potent inhibitors of HLE can clearly be obtained from the  $\beta$ -carbolinone series.

Our initial investigations focused on the tetrahydro- $\beta$ -carbolinone derivatives (Table 1). Molecular modeling

Scheme 6. General Method D<sup>a</sup>

<sup>a</sup> Reagents: (a) **9**, EDC, Et<sub>3</sub>N, DMF; (b) (i) H<sub>2</sub> Pd/C, acetic acid, 80 °C; (ii) <sup>t</sup>BuMe<sub>2</sub>SiCl, imidazole, DMF; (c) (i) H<sub>2</sub> Pd/C, ethanol; (ii) *N*-phenyltrifluoromethanesulfonamide, Et<sub>3</sub>N, CH<sub>2</sub>Cl<sub>2</sub>; (iii) (CH<sub>3</sub>O)<sub>2</sub>P(O)H, 4-methylmorpholine, tetrakis(triphenylphosphine)-palladium(0), acetonitrile; (iv) AlCl<sub>3</sub>, benzene, CH<sub>3</sub>NO<sub>2</sub>; (d) EDC, Cl<sub>2</sub>CHCO<sub>2</sub>H, toluene, DMSO; (e) Bu<sub>4</sub>NF, THF.

indicated that these compounds could bind to HLE so as to access key binding interactions (Figure 2). However, compounds in this class exhibited disappointing levels of *in vitro* activity, as exemplified by **12a–c** (Table 1). Interestingly, even this relatively poor micromolar level of activity was lost for **12a** upon its reduction to the trifluoromethyl alcohol form. This demonstrated that formation of a hemiketal linkage with Ser 195 was an important component of efficient HLE inhibition. With this mechanistic fact established, our goal became the appropriate modification of the  $\beta$ -carbolinone template and its substituents in order to increase *in vitro* potency for the series.

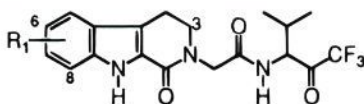
Molecular mechanics energy minimization of **12a** in the active site of HLE revealed that the 8-position of the tetrahydro- $\beta$ -carbolinone template was in proximity to the NH of Gly 218. We hypothesized that the placement of a suitable acceptor functionality at the 8-position might allow for the formation of a hydrogen bond with this NH group. Encouragingly, molecular mechanics minimization of **12d** in the HLE active site showed the formation of the proposed hydrogen-bonding interaction. Experimentally our modeling hypothesis seemed to be strengthened by the observation that the 8-carboxy-substituted compound (**12d**) exhibited a 41-fold increase in binding affinity relative to the unsubstituted compound (**12a**). The dihydro- $\beta$ -carbolinones which, in general, exhibited greater potency than the corresponding tetrahydro derivatives also showed an increase in potency for the 8-carboxy derivative (**13d**) relative to the unsubstituted compound (**13a**). Interestingly, however, molecular mechanics minimization of the 8-ethyl ester (**13e**) and 8-amido (**13f**) dihydro derivatives also showed the formation of a hydrogen bond with Gly 218 *without* a corresponding experimental increase in *in vitro* potency. While **13e** did show geometric distortion upon minimization in the active site as a result of the sterically encumbering 8-position ester, offering a possible explanation for the poor *in vitro* performance of this derivative, the missing *in vitro* potency boost expected for **13f** was bothersome.

Aqueous molecular dynamics (MD) simulations were employed to investigate the binding of these dihydro-

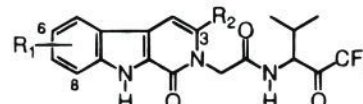
$\beta$ -carbolinones under conditions that more closely represent the experimental environment. MD of the parent dihydro- $\beta$ -carbolinone (**13a**) in HLE showed that the inhibitor was able to maintain all of the critical binding interactions with the enzyme (Figure 3) calculated in our previous molecular mechanics minimizations, including the  $\beta$ -sheet hydrogen-bonding interactions with Val 216. For **13d**, however, the hydrogen-bonding interaction with the NH of Gly 218 was no longer obtained when molecular motion and competing water-inhibitor, water-enzyme interactions were considered. Rather, in addition to the binding interactions observed for **13a**, a relatively long-lived interaction was formed between the 8-carboxylate group of **13d** and the guanidinium group of Arg 177 (Figure 4). Simulations employing **13h**, in which the carboxylate group is moved to the 7-position, revealed that this isomer places the acid functionality beyond the reach of the Arg 177 side chain. While  $\beta$ -sheet hydrogen-bonding interactions remain intact, no guanidinium-carboxylate interactions are noted in simulations for this compound, even when the Arg 177 orientation found for **13d** is employed as the starting geometry. Consistent with these results is the observation that no increase in binding affinity relative to **13a** is observed for **13h** *in vitro*. Similarly, the 8-amido derivative (**13f**) shows no tendency to form a hydrogen bond with Gly 218 NH or stabilizing interaction with Arg 177. The small decrease in potency for **13f** relative to **13a** may be the result of competition by the 8-amido carbonyl for the hydrogen bond from the NH of the  $\beta$ -carbolinone. Such an interaction would weaken the hydrogen bond with the carbonyl oxygen of Val 216, decreasing the *in vitro* potency relative to **13a**. While such competition should also be present in **13d**, the additional stabilizing interaction with Arg 177 may be sufficient to compensate for the small loss from this intramolecular interaction. Aqueous MD simulations for the 8-ethyl ester derivative, **13e**, revealed that one of the crucial hydrogen bonds between the inhibitor ( $\beta$ -carbolinone NH) and Val 216 (carbonyl oxygen) is not well formed, spending greater than half the time at distances longer than one would consider acceptable for efficient hydrogen bond formation ( $N \cdots O > 3.2 \text{ \AA}$ ). No binding interaction is observed with Arg 177 or Gly 218 for **13e**. These binding differences, which are most probably a direct consequence of the greater 8-position steric bulk for this inhibitor, provide a reasonable explanation for the observation that **13e** is a weaker inhibitor than **13a,f,h**. In contrast to the *in vacuo* molecular mechanics minimization results, these MD simulations are, therefore, completely consistent with the observed *in vitro* binding trends obtained for **13a,d–f,h**.

The sp<sup>2</sup> center at the 3-position of the dihydro- $\beta$ -carbolinone template presents a geometry analogous to the 6-position of the previously described pyridone-based HLE inhibitors. This similarity allows for the possibility of directly exploiting the SAR information obtained from this closely related set of inhibitors in the design of more potent dihydro- $\beta$ -carbolinones. For the pyridone class of inhibitors (e.g., **5**, Figure 2), a significant increase in potency results from placing a phenyl substituent at the 6-position of the pyridone ring. X-ray crystallography of a complex between a phenyl-substituted pyridone inhibitor and PPE has revealed

**Table 1.** Physical and Synthetic Data for Tetra- and Dihydrocarbolinones



Tetrahydro Series



Dihydro Series

compd	R <sub>1</sub>	R <sub>2</sub>	Series	HLE K <sub>i</sub> (nM)	molecular formula <sup>a</sup>	mp (°C)	method of preparation <sup>b</sup>
12a	H		tetrahydro	1100 ± 200	C <sub>19</sub> H <sub>20</sub> F <sub>3</sub> N <sub>3</sub> O <sub>3</sub>	199–201	A
12b	6-Cl		tetrahydro	1000 ± 200	C <sub>19</sub> H <sub>19</sub> ClF <sub>3</sub> N <sub>3</sub> O <sub>3</sub>	242	A
12c	6-OCH <sub>3</sub>		tetrahydro	1100 ± 200	C <sub>20</sub> H <sub>22</sub> F <sub>3</sub> N <sub>3</sub> O <sub>4</sub>	244–245	A
12d	8-CO <sub>2</sub> H		tetrahydro	27 ± 4	C <sub>20</sub> H <sub>20</sub> F <sub>3</sub> N <sub>3</sub> O <sub>5</sub>	246	A
13a	H	H	dihydro	290 ± 40	C <sub>19</sub> H <sub>18</sub> F <sub>3</sub> N <sub>3</sub> O <sub>5</sub>	278	A
13b	6-Cl	H	dihydro	210 ± 80	C <sub>19</sub> H <sub>17</sub> ClF <sub>3</sub> N <sub>3</sub> O <sub>3</sub>	293–295	A
13c	6-OCH <sub>3</sub>	H	dihydro	350 ± 60	C <sub>20</sub> H <sub>20</sub> F <sub>3</sub> N <sub>3</sub> O <sub>4</sub> •0.25H <sub>2</sub> O	248–250	A
13d	8-CO <sub>2</sub> H	H	dihydro	22 ± 9	C <sub>20</sub> H <sub>18</sub> F <sub>3</sub> N <sub>3</sub> O <sub>5</sub> •0.25H <sub>2</sub> O	260–262	A or B
13e	8-CO <sub>2</sub> Et	H	dihydro	2500 ± 500	C <sub>22</sub> H <sub>22</sub> F <sub>3</sub> N <sub>3</sub> O <sub>5</sub> •0.33H <sub>2</sub> O	218	A
13f	8-CONH <sub>2</sub>	H	dihydro	730 ± 160	C <sub>20</sub> H <sub>19</sub> F <sub>3</sub> N <sub>4</sub> O <sub>4</sub> •0.3EtOH	316	A
13g	7-CO <sub>2</sub> Et	H	dihydro	340 ± 90	C <sub>22</sub> H <sub>22</sub> F <sub>3</sub> N <sub>3</sub> O <sub>5</sub> •0.6H <sub>2</sub> O	255–256	B
13h	7-CO <sub>2</sub> H	H	dihydro	510 ± 20	C <sub>20</sub> H <sub>18</sub> F <sub>3</sub> N <sub>3</sub> O <sub>5</sub>	281–283	B
19a	H	iPr	dihydro	54 ± 14	C <sub>22</sub> H <sub>24</sub> F <sub>3</sub> N <sub>3</sub> O <sub>3</sub>	256	B
19b	H	Ph	dihydro	6.1 ± 3	C <sub>25</sub> H <sub>22</sub> F <sub>3</sub> N <sub>3</sub> O <sub>3</sub> •0.3H <sub>2</sub> O	317–319	B
19c	8-CN	Ph	dihydro	6.6 ± 1.3	C <sub>26</sub> H <sub>21</sub> F <sub>3</sub> N <sub>4</sub> O <sub>3</sub> •0.6H <sub>2</sub> O <sup>c</sup>	271	B
19d	8-OSO <sub>2</sub> CH <sub>3</sub>	Ph	dihydro	15 ± 2	C <sub>26</sub> H <sub>24</sub> F <sub>3</sub> N <sub>3</sub> O <sub>6</sub> S	255–256	B, D
19e	8-OC(O)OCH <sub>3</sub>	Ph	dihydro	24 ± 5	C <sub>27</sub> H <sub>24</sub> F <sub>3</sub> N <sub>3</sub> O <sub>6</sub>	246–247	B, D
19f	8-OCH <sub>3</sub>	Ph	dihydro	17 ± 1.7	C <sub>26</sub> H <sub>24</sub> F <sub>3</sub> N <sub>3</sub> O <sub>4</sub> •0.25H <sub>2</sub> O	244–246	B
19g	8-CO <sub>2</sub> H	iPr	dihydro	19 ± 0.5	C <sub>23</sub> H <sub>24</sub> O <sub>5</sub> N <sub>3</sub> F <sub>3</sub> •H <sub>2</sub> O	279 (d)	B, C
19h	8-CN	iPr	dihydro	28 ± 1.7	C <sub>23</sub> H <sub>23</sub> F <sub>3</sub> N <sub>4</sub> O <sub>3</sub>	238–240	B
32	8-CHO	Ph	dihydro	4.9 ± 0.2	C <sub>26</sub> H <sub>22</sub> F <sub>3</sub> N <sub>3</sub> O <sub>4</sub> •1.1H <sub>2</sub> O	232	B, C
33	8-CO <sub>2</sub> CH <sub>3</sub>	Ph	dihydro	130 ± 30	C <sub>27</sub> H <sub>24</sub> F <sub>3</sub> N <sub>3</sub> O <sub>5</sub>	228–231	B, C
34	8-CO <sub>2</sub> H	Ph	dihydro	13 ± 1.9	C <sub>26</sub> H <sub>22</sub> F <sub>3</sub> N <sub>3</sub> O <sub>5</sub> •1.0H <sub>2</sub> O	271–274	B, C
38	8-OH	Ph	dihydro	6.7 ± 1.6	C <sub>25</sub> H <sub>22</sub> F <sub>3</sub> N <sub>3</sub> O <sub>4</sub> •0.3H <sub>2</sub> O	344	B, D
39	8-P(O)(OCH <sub>3</sub> ) <sub>2</sub>	Ph	dihydro	52 ± 11	C <sub>27</sub> H <sub>24</sub> F <sub>3</sub> N <sub>3</sub> O <sub>6</sub> P	149–150	B, D
40	6-P(O)(OCH <sub>3</sub> ) <sub>2</sub>	Ph	dihydro	9.6 ± 5	C <sub>27</sub> H <sub>27</sub> F <sub>3</sub> N <sub>3</sub> O <sub>6</sub> P	248–250	B, D

<sup>a</sup> All compounds were analyzed for C,H,N; the results agreed to within ±0.4% of the theoretical values. <sup>b</sup> A general preparation for each type of synthesis is given in the Experimental Section. <sup>c</sup> N: calcd, 11.08; found, 10.62.

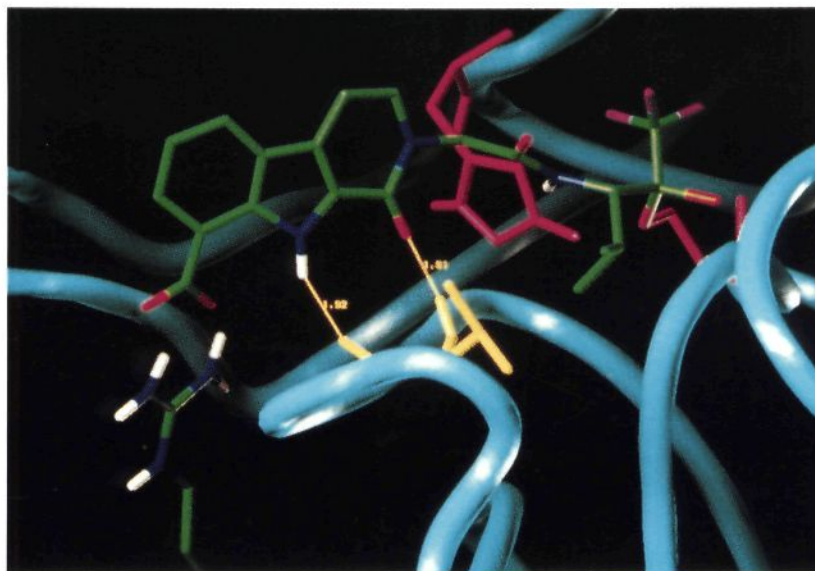


**Figure 4.** One time point from molecular dynamics simulation of **13d** in HLE. Water molecules have been removed for clarity. The enzyme is shown in cyan, His 57 and Ser 195 are shown in red, Val 216 is in yellow, and Arg 177 is in green with nitrogens labeled blue and hydrogens white. The inhibitor **13d** is in green with heteroatoms colored as follows: oxygen—red, nitrogen—blue, hydrogen—white, and fluorine—purple.

that the phenyl moiety is nestled against the S<sub>2</sub> subsite of the enzyme.<sup>19d</sup> Inhibitor **19b** analogously places a phenyl in the 3-position of the β-carbolinone ring, and our aqueous MD simulations on this compound show the phenyl to be bound to the S<sub>2</sub> subsite of HLE.

Experimentally, this compound exhibits a substantial increase in binding affinity (50-fold) relative to **13a**.

We incorporated the two independent ways of increasing the affinity of the β-carbolinone inhibitors for HLE (8-position carboxylate and 3-position phenyl) into one

**Table 2.** Selectivity Data for **13d**

enzyme	$K_i$ (nM)
human leukocyte elastase	22
porcine pancreatic elastase	NI <sup>a</sup>
chymotrypsin (bovine)	NI <sup>a</sup>
trypsin (bovine)	NI <sup>a</sup>
thrombin (human)	NI <sup>a</sup>
AChE (electric eel)	NI <sup>a</sup>
papain	NI <sup>a</sup>
ACE (rabbit)	94 000
cathepsin G (human)	130 000

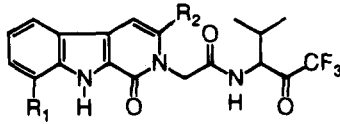
<sup>a</sup> No inhibition at highest concentration tested (400  $\mu$ M).

inhibitor (**34**) in the hope of obtaining a synergistic increase in *in vitro* potency. Interestingly, the  $K_i$  for **34** (13 nM) was found to be *intermediate* between the 8-carboxy (22 nM) and the 3-phenyl (6.1 nM) derivatives. Simulations for **34** show interactions between the carboxylate group and the guanidinium of Arg 177 that are similar to those observed for **13d**. However, while the 3-phenyl of **34** remains proximal to the  $S_2$  region, the aryl group is significantly lifted from the HLE binding site relative to its orientation in **19b**. The prying of the 3-phenyl substituent from the  $S_2$  pocket is a direct geometric consequence of attempting to maintain interactions with Arg 177 at the opposite end of the  $\beta$ -carbolinone template. These simulations qualitatively suggest that **34**, rather than taking full advantage of each of the binding interactions observed for **13d** and **19b**, compromises by maintaining some of binding interactions with Arg 177 while sacrificing a significant portion of the beneficial hydrophobic interactions between the 3-phenyl substituent and the  $S_2$  pocket. For such a binding arrangement, one might reasonably expect to obtain only some of the potency benefit observed for each substituent independently. An intermediate  $K_i$ , as observed, is a reasonable outcome for such a binding orientation. These findings for **34** are also consistent with the experimental observation that the 8-carboxy-tetrahydro- $\beta$ -carbolinone **12d** exhibits a  $K_i$  that is comparable to that observed for **13d**. The emphasis on formation of the binding interaction with Arg 177, and its subsequent geometric requirements, reduces the influence of the geometry and substitution pattern in the 3-position (e.g., tetrahydro vs dihydro) relative to that which pertains for the des-8-carboxy derivatives. Without the 8-carboxy substituent, the  $\beta$ -carbolinones are more sensitive to 3-position geometry and the tetrahydro parent, **12a**, is consequently less potent than the dihydro, **13a**.

In general, the  $\beta$ -carbolinone series of inhibitors was found to have good selectivity for HLE vs a broad range of other proteolytic enzymes (Table 2). One exception to this was the finding that the addition of a 3-position substituent increased binding affinity for bovine pancreatic chymotrypsin, with the 3-phenyl substituent being most problematic.<sup>32</sup> Incorporation of polar 8-position substituents into 3-phenyl-substituted  $\beta$ -carbolinones (e.g., **34** and **39**, Table 3) resulted in substantial improvements in selectivity ratios.

## Pharmacology

Several of the compounds in Table 1 (**13d**, **34**, **38**, and **40**) were evaluated for activity in an acute lung hemorrhagic model<sup>33</sup> after a 30 mg/kg oral dose of inhibitor. This model measures the ability of an orally dosed

**Table 3.** Selectivity Data


compd	$R_1$	$R_2$	$K_i$ (nM)		
			HLE	bovine chymotrypsin	ratio
<b>13a</b>	H	H	290	NI <sup>a</sup>	–
<b>13d</b>	CO <sub>2</sub> H	H	22	NI <sup>a</sup>	–
<b>19a</b>	H	iPr	54	1100	20
<b>19b</b>	H	Ph	6.1	430	70
<b>19c</b>	CN	Ph	6.6	180	27
<b>39</b>	P(O)(OCH <sub>3</sub> ) <sub>2</sub>	Ph	52	26 000	500
<b>34</b>	CO <sub>2</sub> H	Ph	13	43 000	3308

<sup>a</sup> No inhibition at the highest concentrations tested (> 150  $\mu$ M).

inhibitor to protect the lung from hemorrhage induced by the instillation of a 50 unit dose of HLE into the trachea of anesthetized hamsters. The amount of hemorrhage is measured by the spectrophotometric determination of the amount of hemoglobin present in a lung lavage sample taken 3 h postelastase treatment. Disappointingly, none of the compounds showed statistically significant protection against the HLE-induced lung hemorrhage. The lack of oral activity in these compounds could be due to several factors, including poor oral bioavailability, rapid clearance, or poor penetration into the lung from the systemic circulation. To determine if blood levels of inhibitor were being obtained after oral dosing, a 75 mg/kg dose of **13d** was given to hamsters followed by pharmacokinetic determination of plasma levels using our published procedure.<sup>18a</sup> This experiment failed to show detectable levels of functional inhibitor to be present in blood, suggesting poor absorption or extensive first pass metabolism were likely factors responsible for the lack of oral activity.

## Summary

The  $\beta$ -carbolinone family of trifluoromethyl ketone-based inhibitors can exhibit significant *in vitro* potency and selectivity for HLE. Inspection of X-ray crystallographic results and molecular mechanics modeling were helpful in both the initial design of this class of inhibitor and in developing suggestions for substitution patterns that would improve *in vitro* potency. In some cases, results from *in vacuo* molecular mechanics minimizations provided results that were inconsistent with experimental observation. This most probably results from these minimizations not considering the influence of molecular motion and inadequately representing the effect of molecular solvation. Aqueous MD simulations were able to provide representations of inhibitor-binding interactions with HLE that are consistent with experimental binding results. These simulations reveal the potential importance of interactions between 8-carboxy-substituted  $\beta$ -carbolinones and Arg 177.

## Experimental Section

**General Methods.** Analytical samples were homogeneous by TLC and afforded spectroscopic results consistent with the assigned structures. Proton NMR spectra were obtained using either a Bruker WM-250 or AM-300 spectrometer. Chemical shifts are reported in parts per million relative to Me<sub>4</sub>Si as internal standard. Mass spectra (MS) were recorded on a Kratos MS-80 instrument operating in the chemical ionization

(CI) mode. Elemental analyses for carbon, hydrogen, and nitrogen were determined by the ZENEGA Pharmaceuticals Analytical Department on a Perkin-Elmer 241 elemental analyzer and are within  $\pm 0.4\%$  of theory for the formulas given. Analytical thin-layer chromatography (TLC) was performed on precoated silica gel plates (60F-254, 0.2 mm thick; E. Merck). Visualization of the plates was accomplished by using UV light or phosphomolybdic acid/ethanol-charring procedures. Chromatography refers to flash chromatography conducted on Kieselgel 60, 230–400 mesh (E. Merck, Darmstadt) using the indicated solvents. Solvents used for reactions or chromatography were either reagent grade or HPLC grade. Reactions were run under an argon atmosphere at ambient temperature unless otherwise noted. Solutions were evaporated under reduced pressure on a rotary evaporator. The following abbreviations are used, THF, tetrahydrofuran; DMF, *N,N*-dimethylformamide; DMSO, dimethyl sulfoxide; EDC, 1-[3-(dimethylamino)propyl]-3-ethylcarbodiimide hydrochloride; TFA, trifluoroacetic acid; DPPA, diphenyl phosphorazidate; Suc, succinyl; pNA, *p*-nitroaniline; DDQ, 2,3-dichloro-5,6-dicyano-1,4-benzoquinone.

**General Method A. 1-Oxo-9-[[2-(trimethylsilyl)ethoxy]methyl]-1,2,3,4-tetrahydropyrido[3,4-*b*]indole (8;  $R_1 = H$ ).** To a solution of **7** (1.86 g, 10 mmol) in dry THF (200 mL) was added NaH (0.5 g, 12 mmol of a 60% dispersion in oil), and the reaction mixture was stirred for 0.5 h. [2-(Trimethylsilyl)ethoxy]methyl chloride (2.5 mL, 14 mmol) was added and the resulting solution allowed to stir for an additional 16 h. The reaction was quenched by addition of saturated aqueous ammonium chloride and the product then extracted into ethyl acetate. The organic layer was washed with saturated sodium bicarbonate, H<sub>2</sub>O, and brine. The solution was dried (MgSO<sub>4</sub>) and the solvent removed. The resulting oil was chromatographed (gradient elution, 30% ethyl acetate/hexanes to 50% ethyl acetate/hexanes) to provide **8** (2.6 g, 82%) as a white solid: <sup>1</sup>H NMR (300 MHz, DMSO)  $\delta$  7.71 (s, 1H), 7.65 (d,  $J = 8$  Hz, 1H), 7.60 (d,  $J = 8.4$  Hz, 1H), 7.33 (t,  $J = 7.7$  Hz, 1H), 7.16 (t,  $J = 7.5$  Hz, 1H), 6.01 (s, 2H), 3.45 (m, 4H), 2.94 (t,  $J = 6.8$  Hz, 2H), 0.77 (t,  $J = 6.8$  Hz, 2H), -0.12 (s, 9H).

***N*-[2-[(*tert*-Butyldimethylsilyl)oxy]-3,3,3-trifluoro-1-isopropylpropyl]-2-iodoacetamide (10).** To a solution of 3-amino-1,1,1-trifluoro-4-methyl-2-pentanol hydrochloride (**9**; 20 g, 97 mmol) in dry THF (480 mL) was added 4-methylmorpholine (21.8 mL, 198 mmol) followed by slow addition of a solution of chloroacetyl chloride (7.7 mL, 97 mmol in 40 mL of THF). The resulting solution was allowed to stir overnight, after which time it was diluted with ethyl acetate and filtered free of undissolved solids. The filtrate was washed with 1 N HCl, H<sub>2</sub>O, saturated aqueous sodium bicarbonate, and brine. The solution was dried (MgSO<sub>4</sub>) and the solvent removed to provide the crude amide as an oil. The crude amide was dissolved in dichloromethane (96 mL) and 2,6-lutidine (22.5 mL, 193 mmol) added. To this solution was added *tert*-butyldimethylsilyl triflate (33 mL, 143 mmol) followed by stirring for 12 h. The solution was diluted with ethyl acetate and washed with 1 N HCl (2 $\times$ ), saturated sodium bicarbonate, and brine. The ethyl acetate solution was adsorbed onto silica gel (120 mL) by evaporation and chromatographed (gradient elution, 7% ethyl acetate/hexanes to 20% ethyl acetate/hexanes) to afford the silylated material (20.5 g) as a white solid. A portion of this material (15.5 g, 43 mmol) was dissolved in acetone (130 mL), and NaI (19.3 g, 128 mmol) was added followed by stirring overnight at room temperature. The solution was diluted with H<sub>2</sub>O, and the resulting precipitate was filtered and washed with saturated aqueous sodium thiosulfate and H<sub>2</sub>O. The solid was dried under vacuum followed by chromatography (gradient elution, 20% ethyl acetate/hexanes to 50% ethyl acetate/hexanes) to provide **10** (17.9 g, 41%) as a white solid: <sup>1</sup>H NMR (300 MHz, DMSO)  $\delta$  6.51 (d,  $J = 10$  Hz, 1H), 4.15 (q,  $J = 6.6$  Hz, 1H), 3.74 (s, 2H), 1.76 (m, 1H), 0.96 (m, 15H), 0.16 (s, 3H), 0.12 (s, 3H); MS (CI) 454 (M + H).

**1-Oxo-9-[[2-(trimethylsilyl)ethoxy]methyl]-1,2,3,4-tetrahydropyrido[3,4-*b*]indol-2-yl]-*N*-[2-[(*tert*-butyldimethylsilyl)oxy]-3,3,3-trifluoro-1-isopropylpropyl]acetamide (11;  $R_1 = H$ ).** To a solution of **8** (2.6 g, 7.8 mmol) in dry

THF (200 mL) was added NaH (0.4 g, 10 mmol of a 60% dispersion in oil) followed by stirring for 0.5 h. A solution of **10** (3.6 g, 8 mmol in 25 mL of THF) was added and the reaction mixture stirred for 16 h. The reaction was quenched with saturated ammonium chloride and the product extracted into ethyl acetate. The organic layer was washed with saturated sodium bicarbonate, H<sub>2</sub>O, and brine. The solution was dried (MgSO<sub>4</sub>) and the solvent removed. The resulting oil was chromatographed (25% ethyl acetate/petroleum ether) to give **11** (3.95 g, 79%) as a colorless oil: <sup>1</sup>H NMR (300 MHz, DMSO)  $\delta$  7.65 (d,  $J = 7.9$  Hz, 1H), 7.60 (d,  $J = 8.4$  Hz, 1H), 7.34 (t,  $J = 7.7$  Hz, 1H), 7.25 (d,  $J = 9.7$  Hz, 1H), 7.17 (t,  $J = 7.8$  Hz, 1H), 5.99 (m, 2H), 4.38 (m, 2H), 4.22 (d,  $J = 16.3$  Hz, 1H), 4.11 (d,  $J = 16.2$  Hz, 1H), 3.85 (t,  $J = 8$  Hz, 1H), 3.66 (m, 2H), 3.46 (t,  $J = 7.9$  Hz, 2H), 3.03 (t,  $J = 6.9$  Hz, 2H), 1.73 (m, 1H), 0.95 (d,  $J = 6.6$  Hz, 3H), 0.88 (d,  $J = 6.7$  Hz, 3H), 0.78 (s, 9H), 0.11 (s, 3H), 0.09 (s, 3H), -0.12 (s, 9H).

**(1-Oxo-1,2,3,4-tetrahydropyrido[3,4-*b*]indol-2-yl)-*N*-(3,3,3-trifluoro-1-isopropyl-2-oxopropyl)acetamide (12;  $R_1 = H$ ).** A solution of **11** (3.95 g, 6 mmol) in THF (12 mL) containing *tetra*-butylammonium fluoride (12 mmol) was refluxed for 5 h. The reaction mixture was poured into saturated ammonium chloride and the product extracted into ethyl acetate. The organic phase was washed with saturated sodium bicarbonate and brine and then dried (MgSO<sub>4</sub>). The solvent was removed and the resulting brown solid chromatographed (gradient elution, 50% ethyl acetate/petroleum ether to 100% ethyl acetate) to yield the desired alcohol (**2** g, 84%) as a white solid: <sup>1</sup>H NMR (250 MHz, DMSO)  $\delta$  11.6 (s, 1H), 7.68 (d,  $J = 9.7$  Hz, 1H), 7.60 (d,  $J = 8.0$  Hz, 1H), 7.40 (d,  $J = 8.8$  Hz, 1H), 7.22 (t,  $J = 7.7$  Hz, 1H), 7.06 (d,  $J = 7.5$  Hz, 1H), 6.55 (d,  $J = 6.9$  Hz, 1H), 4.17 (m, 2H), 3.89 (t,  $J = 9.0$  Hz, 1H), 3.67 (m, 2H), 3.01 (t,  $J = 6.9$  Hz, 2H), 1.82 (m, 1H), 0.92 (d,  $J = 6.6$  Hz, 3H), 0.88 (d,  $J = 6.8$  Hz, 3H).

To a solution of this alcohol (1.59 g, 4 mmol) in toluene (20 mL) and DMSO (20 mL) were added 1-[3-(dimethylamino)propyl]-3-ethylcarbodiimide (7.7 g, 40 mmol) and then dichloroacetic acid (1.3 mL, 16 mmol). After stirring for 2 h, the reaction mixture was diluted with ethyl acetate and washed with saturated ammonium chloride, saturated sodium bicarbonate, H<sub>2</sub>O, and brine. The solution was dried (MgSO<sub>4</sub>) and the solvent removed. The resulting material was chromatographed (50% ethyl acetate/petroleum ether) and the product recrystallized from ethyl acetate to provide **12** as a white solid (0.64 g, 40%): mp 199.5–201 °C; <sup>1</sup>H NMR (250 MHz, DMSO)  $\delta$  11.6 (s, 1H), 8.72 (d,  $J = 6.6$  Hz, 1H), 7.59 (d,  $J = 7.4$  Hz, 1H), 7.39 (d,  $J = 8.0$  Hz, 1H), 7.22 (t,  $J = 7.3$  Hz, 1H), 7.06 (t,  $J = 7.5$  Hz, 1H), 4.62 (t,  $J = 6.3$  Hz, 1H), 4.24 (m, 2H), 3.71 (t,  $J = 6.9$  Hz, 2H), 3.00 (t,  $J = 6.9$  Hz, 2H), 2.20 (m, 1H), 0.96 (d,  $J = 6.4$  Hz, 3H), 0.93 (d,  $J = 6.5$  Hz, 3H). Anal. (C<sub>19</sub>H<sub>20</sub>F<sub>3</sub>N<sub>3</sub>O<sub>3</sub>) C, H, N.

**(1-Oxo-1,2-dihydropyrido[3,4-*b*]indol-2-yl)-*N*-(3,3,3-trifluoro-1-isopropyl-2-oxopropyl)acetamide (13;  $R_1 = H$ ).** To a solution of **12** (1.0 g, 2.5 mmol) in dioxane (25 mL) was added DDQ (1.7 g, 7.5 mmol), and the resulting mixture was stirred for 1 h. The reaction mixture was diluted with ethyl acetate and washed with saturated sodium bicarbonate, H<sub>2</sub>O, and brine. The solution was dried (MgSO<sub>4</sub>) and the solvent evaporated. The resulting solid was chromatographed (ethyl acetate) and then recrystallized from ethyl acetate to provide **13** (0.38 g, 39%) as a white solid: mp 278 °C dec; <sup>1</sup>H NMR (250 MHz, DMSO)  $\delta$  11.9 (s, 1H), 8.93 (d,  $J = 6.6$  Hz, 1H), 8.03 (d,  $J = 7.9$  Hz, 1H), 7.53 (d,  $J = 8.2$  Hz, 1H), 7.42 (t,  $J = 7.4$  Hz, 1H), 7.32 (d,  $J = 7.0$  Hz, 1H), 7.19 (t,  $J = 7.4$  Hz, 1H), 7.02 (d,  $J = 7.0$  Hz, 1H), 4.85 (m, 2H), 4.66 (t,  $J = 6.3$  Hz, 1H), 2.22 (m, 1H), 0.98 (d,  $J = 6.8$  Hz, 3H), 0.96 (d,  $J = 6.7$  Hz, 3H). Anal. (C<sub>19</sub>H<sub>18</sub>F<sub>3</sub>N<sub>3</sub>O<sub>3</sub>) C, H, N.

**General Method B. *N*-Allyl-1-benzyl-7-cyano-*N*-(2,2-diethoxy-1-phenylethyl)-2-indolecarboxamide (15;  $R_1 = 7-CN$ ,  $R_2 = Ph$ ,  $R_3 = allyl$ ).** To a solution of **14** (7.3 g, 26 mmol) in dichloromethane (90 mL) at room temperature were added oxalyl chloride (4.6 mL, 53 mmol) and *N,N*-dimethylformamide (0.1 mL). The resulting solution was allowed to stir for 1 h, and then the solvent was evaporated. The residue was dissolved in dichloromethane (60 mL) and cooled to 0 °C, and to this were added **25** (9.6 g, 39 mmol) and triethylamine



(7.3 mL, 53 mmol) followed by stirring overnight. The reaction mixture was then diluted with ethyl acetate and washed with 1 N HCl, H<sub>2</sub>O, and brine followed by drying (MgSO<sub>4</sub>) and evaporation of the solvent. The crude material was purified by chromatography (30% ether/hexanes) to afford **15** (10.5 g, 80%) as an oil: MS (CI) 508 (M + H).

**2-Allyl-9-benzyl-8-cyano-3-phenylpyrido[3,4-*b*]indol-1(2*H*)-one (16; R<sub>1</sub> = 7-CN, R<sub>2</sub> = Ph, R<sub>3</sub> = allyl).** To a solution of **15** (10.4 g, 20 mmol) in ether (200 mL) at 25 °C was added concentrated sulfuric acid (3 mL), and the resulting solution was stirred for 3 h. The reaction was quenched by addition of saturated aqueous sodium bicarbonate (100 mL) and the product extracted into ethyl acetate. The solution was dried (MgSO<sub>4</sub>) and the solvent removed to give a yellow solid. This solid was collected and washed several times with hexane to give **16** (7.5 g, 90%) as a yellow solid: <sup>1</sup>H NMR (300 MHz, DMSO) δ 8.56 (d, *J* = 9 Hz, 1H), 7.96 (d, *J* = 6 Hz, 1H), 7.52 (s, 5H), 7.37 (t, *J* = 9 Hz, 1H), 7.28 (m, 5H), 7.21 (s, 1H), 6.97 (d, *J* = 6.9 Hz, 2H), 5.75 (m, 1H), 5.0 (d, *J* = 10 Hz, 1H), 4.7 (d, *J* = 15 Hz, 1H), 4.57 (br s, 2H); MS (CI) 416 (M + H).

**(9-Benzyl-8-cyano-1-oxo-3-phenyl-1,2-dihydropyrido[3,4-*b*]indol-2-yl)acetic Acid (17; R<sub>1</sub> = 7-CN, R<sub>2</sub> = Ph).** To a solution of **16** (1.09 g, 2.6 mmol) in tetrahydrofuran (26 mL) and H<sub>2</sub>O (3 mL) were added *N*-methylmorpholine *N*-oxide (0.34 g, 2.9 mmol) and a catalytic amount of osmium tetroxide (0.1 mL of a 4% solution in H<sub>2</sub>O). The resulting solution was allowed to stir overnight. The reaction was quenched by addition of saturated aqueous Na<sub>2</sub>S<sub>2</sub>O<sub>3</sub> and the product filtered through Celite. The solvent was evaporated; the residue was diluted with ethyl acetate and washed with 1 N HCl and H<sub>2</sub>O. The solution was evaporated and the resulting material dissolved in ethanol (30 mL), and to this was added sodium periodate (0.73 g, 3.4 mmol) in H<sub>2</sub>O (10 mL) followed by stirring for 2 h. The solvent was evaporated. The residue was diluted with ethyl acetate, washed with H<sub>2</sub>O, and dried (MgSO<sub>4</sub>) and the solvent removed to give the crude aldehyde. This material was dissolved in tetrahydrofuran (10 mL), *tert*-butyl alcohol (25 mL), and 2-methyl-2-butene (5.8 mL) followed by cooling to 0 °C. A solution of sodium chlorite (3.15 g, 25 mmol) and sodium dihydrogen phosphate monohydrate (2.64 g, 19 mmol) in H<sub>2</sub>O (10 mL) was added followed by stirring for 0.5 h. The reaction was quenched by addition of saturated aqueous Na<sub>2</sub>S<sub>2</sub>O<sub>3</sub> and the solvent evaporated. The residue was dissolved in H<sub>2</sub>O, the pH adjusted to pH 3 with 1 N HCl, and the product extracted into dichloromethane. The organic extracts were dried (MgSO<sub>4</sub>) and the solvent removed to give an oil which crystallized upon addition of ether to give **17** (0.88 g, 81%) as a yellow solid: <sup>1</sup>H NMR (300 MHz, DMSO) δ 8.60 (d, *J* = 9 Hz, 1H), 8.00 (d, *J* = 9 Hz, 1H), 7.52 (m, 5H), 7.42 (t, *J* = 9 Hz, 1H), 7.26 (m, 6H), 7.01 (d, *J* = 6 Hz, 2H), 4.55 (s, 2H); MS (CI) 418 (M + H).

**2-(8-Cyano-1-oxo-3-phenyl-1,2-dihydropyrido[3,4-*b*]indol-2-yl)-*N*-(3,3,3-trifluoro-2-hydroxy-1-isopropylpropyl)acetamide (18; R<sub>1</sub> = 7-CN, R<sub>2</sub> = Ph).** To a solution of **17** (0.9 g, 2.1 mmol), 3-amino-4-methyl-1,1,1-trifluoro-2-pentanone hydrochloride salt (**9**; 0.65 g, 3.1 mmol), 1-hydroxybenzotriazole (0.57 g, 4.2 mmol), and triethylamine (0.6 mL, 4.2 mmol) in DMF (10 mL) was added 1-[3-(dimethylamino)propyl]-3-ethylcarbodiimide (0.5 g, 2.6 mmol), and the resulting solution was allowed to stir overnight. The reaction mixture was poured into ether and washed sequentially with 1 N HCl, 1 N NaOH, and H<sub>2</sub>O. The solution was dried and the solvent evaporated to give a yellow oil which crystallized to give the desired alcohol (0.9 g, 73%) as a yellow solid: <sup>1</sup>H NMR (300 MHz, DMSO) δ 8.58 (d, *J* = 9 Hz, 1H), 7.97 (m, 3H), 7.80 (d, *J* = 9 Hz, 1H), 7.45 (m, 5H), 7.26 (m, 5H), 7.18 (s, 1H), 7.01 (d, *J* = 6 Hz, 2H), 6.45 (d, *J* = 9 Hz, 1H), 4.55 (m, 2H), 4.10 (m, 1H), 3.83 (t, *J* = 9 Hz, 1H), 1.75 (m, 1H), 0.89 (d, *J* = 9 Hz, 3H), 0.79 (d, *J* = 9 Hz, 3H); MS (CI) 587 (M + H).

To a solution of the alcohol (2.0 g, 3.4 mmol) in benzene (15 mL) and nitromethane (5 mL) at room temperature was added aluminum chloride (1.81 g, 13 mmol), and the resulting mixture was allowed to stir for 1 h. The reaction mixture was poured into H<sub>2</sub>O and the product extracted into dichloromethane. The organic extracts were dried (MgSO<sub>4</sub>) and the solvent evaporated. The resulting material was purified by

chromatography (5% methanol/dichloromethane) to give **18** (1.4 g, 83%) as a white solid: <sup>1</sup>H NMR (250 MHz, DMSO) δ 12.9 (s, 1H), 8.47 (d, *J* = 7 Hz, 1H), 7.94 (d, *J* = 7 Hz, 1H), 7.80 (d, *J* = 10 Hz, 1H), 7.47 (m, 5H), 7.34 (t, *J* = 7 Hz, 1H), 7.07 (s, 1H), 6.48 (d, *J* = 6 Hz, 1H), 4.61 (m, 2H), 4.10 (t, *J* = 7 Hz, 1H), 3.84 (t, *J* = 7 Hz, 1H), 1.75 (m, 1H), 0.91 (d, *J* = 7 Hz, 3H), 0.83 (d, *J* = 7 Hz, 3H); MS (CI) 497 (M + H).

**2-(8-Cyano-1-oxo-3-phenyl-1,2-dihydropyrido[3,4-*b*]indol-2-yl)-*N*-(3,3,3-trifluoro-1-isopropyl-2-oxopropyl)acetamide (19; R<sub>1</sub> = 7-CN, R<sub>2</sub> = Ph).** To a solution of **18** (0.3 g, 0.7 mmol) in DMSO (2 mL) and toluene (2 mL) were added 1-[3-(dimethylamino)propyl]-3-ethylcarbodiimide (1.4 g, 7.2 mmol) and dichloroacetic acid (0.23 mL, 2.9 mmol), and the resulting solution was allowed to stir for 2 h at room temperature. The reaction mixture was poured into ethyl acetate and washed several times with 1 N HCl and then H<sub>2</sub>O. The solution was dried (MgSO<sub>4</sub>) and the solvent evaporated. The resulting material was chromatographed (3% methanol/dichloromethane) to give **19** (0.23 g, 67%) as a yellow solid: <sup>1</sup>H NMR (250 MHz, DMSO/D<sub>2</sub>O) δ 8.40 (d, *J* = 7.5 Hz, 1H), 7.91 (d, *J* = 7.5 Hz, 1H), 7.42 (s, 5H), 7.33 (t, *J* = 7.5 Hz, 1H), 7.02 (s, 1H), 4.59 (m, 2H), 4.01 (br s, 1H), 2.18 (m, 1H), 0.80 (d, *J* = 6.8 Hz, 3H), 0.74 (d, *J* = 6.8, 3H); MS (CI) 495 (M + H). Anal. (C<sub>26</sub>H<sub>21</sub>O<sub>3</sub>N<sub>4</sub>F<sub>3</sub>·0.6H<sub>2</sub>O) C, H, N.

**Ethyl 4-Succinoylpyrrole-2-carboxylate (21).** To a solution of ethyl pyrrole-2-carboxylate (35.4 g, 0.255 mol) and succinic anhydride (51 g, 0.51 mol) in nitromethane (500 mL) at 0 °C was added aluminum chloride (136 g, 1.02 mol) portionwise. The resulting mixture was allowed to warm to room temperature and stir for 1 h. The solution was poured into ice/H<sub>2</sub>O (2 L), and a white precipitate formed, which was collected and washed with 1 N HCl and H<sub>2</sub>O. The material was recrystallized from H<sub>2</sub>O to give **21** (50.7 g, 41%) as a white solid: <sup>1</sup>H NMR (300 MHz, DMSO) δ 12.5 (s, 1H), 12.1 (s, 1H), 7.75 (s, 1H), 7.13 (s, 1H), 4.27 (q, *J* = 7.2 Hz, 2H), 3.02 (t, *J* = 6 Hz, 2H), 2.50 (t, *J* = 6 Hz, 2H), 1.29 (t, *J* = 7 Hz, 3H).

**Ethyl 7-Oxo-4,5,6,7-tetrahydroindole-2-carboxylate (22).** To a solution of **21** (41.5 g, 0.17 mol) in acetic acid (1.35 L) and trifluoroacetic acid (0.15 L) was placed 10% Pd/C, and the mixture was shaken under a hydrogen atmosphere (50 psi) overnight. The solution was filtered free of catalyst and the solvent removed. Toluene (300 mL) was added to the residue and then evaporated (3×) to remove residual traces of acetic acid. This gave the desired acid (42 g) sufficiently pure for further use. A portion of this acid (29.2 g, 0.13 mol) was dissolved in trifluoroacetic acid (250 mL), and to this was added trifluoroacetic anhydride (18.4 mL, 0.13 mol) followed by stirring for 3 h. Excess trifluoroacetic acid was removed by evaporation followed by addition of toluene (300 mL) and repeated evaporation. The residue was dissolved in ether and washed with saturated aqueous sodium bicarbonate and H<sub>2</sub>O. The solution was dried (MgSO<sub>4</sub>) and the solvent removed. The resulting solid was recrystallized from ether to provide **22** as an off-white solid (22 g, 82%): <sup>1</sup>H NMR (250 MHz, DMSO) δ 12.4 (s, 1H), 6.66 (br s, 1H), 4.26 (q, *J* = 7 Hz, 2H), 2.68 (t, *J* = 6 Hz, 2H), 2.48 (t, *J* = 5 Hz, 2H), 2.00 (m, 2H), 1.28 (t, *J* = 7 Hz, 3H).

**1-Benzyl-7-cyanoindole-2-carboxylic Acid (23).** To a solution of **22** (18.3 g, 89 mmol) in benzene (50 mL) at room temperature was added trimethylsilyl cyanide (13 mL, 98 mmol) and zinc iodide (0.7 g, 2 mmol). The resulting solution was allowed to stir for 4 h and then diluted with pyridine (125 mL). Phosphorus oxychloride (25 mL, 267 mmol) was added, and the solution was heated at 80 °C for 3 h, cooled to room temperature, poured carefully into a solution of ice/1 N HCl, and extracted into ether. The ether solution was dried (MgSO<sub>4</sub>) and the solvent removed. The crude material was dissolved in dioxane (200 mL) and 2,3-dichloro-5,6-dicyano-1,4-benzoquinone (DDQ) (22 g, 98 mmol) was added. After stirring for 3 h, the mixture was poured into ether and washed with saturated aqueous sodium bicarbonate and brine. The solution was dried (MgSO<sub>4</sub>) and the solvent evaporated. The resulting material was purified by chromatography (50% ether/hexanes) to provide the indole (15 g, 79%) as an off-white solid: <sup>1</sup>H NMR (300 MHz, DMSO) δ 8.06 (d, *J* = 6 Hz, 1H), 7.81 (d, *J* = 7.5 Hz, 1H), 7.34 (br s, 1H), 7.25 (t, *J* = 6 Hz,

1H), 4.37 (q,  $J = 7.2$  Hz, 2H), 1.35 (t,  $J = 6.9$  Hz, 3H); MS (CI) 215 (M + H).

To a solution of the indole (0.54 g, 2.5 mmol) in DMF (10 mL) was added NaH (0.16 g, 3.9 mmol of a 60% dispersion in oil), and the solution was stirred for 1 h. Benzyl bromide (0.33 mL, 2.8 mmol) was added to the solution, and the mixture was allowed to stir overnight. The solution was poured into saturated aqueous ammonium chloride and extracted with ether. The ether layer was washed with 1 N HCl, H<sub>2</sub>O, and brine. The solution was dried (MgSO<sub>4</sub>) and the solvent removed to give an oil which was dissolved in THF (4 mL), methanol (2 mL), and H<sub>2</sub>O (2 mL). Lithium hydroxide (0.18 g, 4.5 mmol) was added. After 1 h, the solvent was removed and the residue diluted with H<sub>2</sub>O and made acidic to pH 2 by addition of 1 N HCl. The product was extracted into ethyl acetate, the solution dried (MgSO<sub>4</sub>), and the solvent removed to provide pure **23** (0.38 g, 56%) as a white solid: <sup>1</sup>H NMR (300 MHz, DMSO)  $\delta$  13.4 (s, 1H) 8.12 (d,  $J = 5.4$  Hz, 1H), 7.81 (d,  $J = 5.7$  Hz, 1H), 7.55 (s, 1H), 7.28 (m, 4H), 6.86 (d,  $J = 6$  Hz, 2H), 6.22 (s, 2H).

**N-Allyl-2,2-diethoxy-1-phenylethylamine (25).** 2,2-Diethoxyacetophenone (40.4 mL, 0.2 mol), allylamine (45 mL, 0.6 mol), acetic acid (17.1 mL, 0.3 mol), and activated 3 Å molecular sieves were combined in ethanol (500 mL), and the mixture was stirred for 1 h. NaBH<sub>3</sub>CN was added followed by stirring for 2 days at room temperature. The reaction mixture was made basic to pH 10 with 1 N NaOH and the solution filtered through Celite. The solvent was evaporated and the resulting material diluted with ether, washed with 1 N NaOH, and then dried (MgSO<sub>4</sub>). The resulting yellow oil was distilled (bp 115 °C, 1.5 mmHg) to provide pure **25** (36.5 g, 49%) as a yellow oil: <sup>1</sup>H NMR (250 MHz, DMSO/TFA)  $\delta$  7.27 (m, 5H), 5.79 (m, 1H), 5.00 (m, 2H), 4.39 (d,  $J = 6.7$  Hz, 1H), 3.65 (m, 2H), 3.46 (m, 2H), 3.13 (m, 1H), 2.92 (m, 2H), 1.14 (t,  $J = 7.5$  Hz, 3H), 0.85 (t,  $J = 7.0$  Hz, 3H).

**N-[(Ethoxycarbonyl)methyl]-2,2-diethoxy-1-isopropylethylamine (29).** To a solution of valinal diethyl acetal (10 g, 58 mmol) and triethylamine (16 mL, 116 mmol) in THF (60 mL) at 0 °C was added ethyl bromoacetate (7.1 mL, 64 mmol), and the resulting mixture was stirred for 24 h, over which time the solution was warmed to room temperature. An additional amount of ethyl bromoacetate (7.1 mL, 64 mmol) was added, and the reaction mixture was stirred for another 16 h. The solution was filtered free of solids and the solvent removed. The resulting oil was chromatographed (20% ethyl acetate/dichloromethane) to afford pure **29** (13 g, 43%) as an oil: <sup>1</sup>H NMR (250 MHz, DMSO)  $\delta$  4.31 (d,  $J = 6$  Hz, 1H), 4.09 (q,  $J = 7$  Hz, 2H), 3.48 (m, 6H), 2.35 (m, 1H), 1.82 (m, 2H), 1.07 (m, 9H), 0.92 (d,  $J = 7$  Hz, 3H), 0.82 (d,  $J = 7$  Hz, 3H); MS (CI) 262 (M + H).

**General Method C. 2-(8-Formyl-1-oxo-3-phenyl-1,2-dihydropyridol[3,4-*b*]indol-2-yl)-N-(2-hydroxy-3,3,3-trifluoro-1-isopropylpropyl)acetamide (30; R<sub>1</sub> = CHO, R<sub>2</sub> = Ph).** To a solution of **18** (0.5 g, 2.5 mmol) and sodium hypophosphite monohydrate (0.35 g, 4 mmol) in pyridine (3 mL), acetic acid (1.5 mL), and H<sub>2</sub>O (1.5 mL) was added a small amount of Raney nickel (50% slurry in water, pH >9), and the resulting mixture was heated at 60 °C for 1 h. Additional sodium hypophosphite monohydrate (0.1 g, 1.1 mmol) was added and the mixture heated at 60 °C for an additional 1 h. The reaction mixture was diluted with methanol, filtered through Celite, evaporated, and diluted with ethyl acetate. The resulting solution was washed with 1 N HCl, dried (MgSO<sub>4</sub>), and evaporated to obtain a yellow solid. This material was chromatographed (gradient elution, 5% methanol/dichloromethane to 10% methanol/dichloromethane) to provide **30** (0.4 g, 32%) as a yellow solid: <sup>1</sup>H NMR (250 MHz, DMSO)  $\delta$  11.98 (s, 1H), 10.58 (s, 1H), 8.47 (d,  $J = 7.7$  Hz, 1H), 8.02 (d,  $J = 7.3$  Hz, 1H), 7.82 (d,  $J = 9.5$  Hz, 1H), 7.44 (m, 7H), 7.10 (s, 1H), 6.50 (d,  $J = 6.2$ , 1H), 4.50 (m, 2H), 4.10 (m, 1H), 3.84 (t,  $J = 8.7$  Hz, 1H), 1.78 (m, 1H), 0.91 (t,  $J = 6.6$  Hz, 3H), 0.83 (t,  $J = 6.5$  Hz, 3H); MS (CI) 500 (M + H).

**2-[8-(Methoxycarbonyl)-1-oxo-3-phenyl-1,2-dihydropyridol[3,4-*b*]indol-2-yl)-N-(3,3,3-trifluoro-2-hydroxy-1-isopropylpropyl)acetamide (31; R<sub>1</sub> = CO<sub>2</sub>CH<sub>3</sub>, R<sub>2</sub> = Ph).** To a solution of **30** (0.26 g, 0.62 mmol) in *tert*-butyl alcohol (7 mL),

THF (3 mL), and 2-methyl-2-butene (1.3 mL) was added a solution of sodium chlorite (0.5g, 5.6 mmol) and sodium dihydrogen phosphate (0.61 g, 4.4 mmol) in H<sub>2</sub>O (2 mL). The resulting solution was allowed to stir for 0.5 h and the solvent removed by evaporation. The residue was diluted with H<sub>2</sub>O and made acidic to pH 3 by addition of 1 N HCl. The solution was extracted with dichloromethane, and the organic layers were dried and evaporated. The residue was dissolved in ether (10 mL) and methanol (3 mL) and treated with ethereal diazomethane until a yellow color persisted. The excess diazomethane was quenched by addition of acetic acid and the solvent evaporated. The resulting material was chromatographed (1% methanol/dichloromethane) to provide **31** (0.185 g, 48%) as an off-white solid: <sup>1</sup>H NMR (250 MHz, DMSO)  $\delta$  8.42 (d,  $J = 7.8$  Hz, 1H), 7.82 (d,  $J = 9.5$  Hz, 1H), 7.69 (d,  $J = 7.5$  Hz, 1H), 7.47 (m, 5H), 7.28 (t,  $J = 7.5$  Hz, 1H), 7.13 (m, 5H), 6.73 (d,  $J = 7.5$  Hz, 2H), 6.45 (d,  $J = 7$  Hz, 1H), 6.40 (br s, 1H), 4.62 (m, 2H), 4.08 (m, 1H), 3.83 (m, 1H), 3.77 (s, 3H), 1.76 (m, 1H), 0.89 (d,  $J = 6.5$  Hz, 3H), 0.80 (d,  $J = 6.8$  Hz, 3H); MS (CI) 620 (M + H).

**2-(8-Carboxy-1-oxo-3-phenyl-1,2-dihydropyridol[3,4-*b*]indol-2-yl)-N-(3,3,3-trifluoro-1-isopropyl-2-oxopropyl)acetamide (34; R<sub>2</sub> = Ph).** To a solution of **33** (0.17 g, 0.32 mmol) in THF (7 mL) and H<sub>2</sub>O (1.5 mL) was added lithium hydroxide monohydrate (0.04 g), and the resulting solution was allowed to stir for 1 h. The solution was made acidic to pH 3 by addition of 1 N HCl and the product extracted into dichloromethane. The organic layers were dried (MgSO<sub>4</sub>), and the solvent was removed. The material was purified by chromatography (gradient elution, 5% methanol/dichloromethane to 10% methanol/dichloromethane) to provide **34** (0.1 g, 61%) as a tan solid: <sup>1</sup>H NMR (250 MHz, DMSO/D<sub>2</sub>O)  $\delta$  8.13 (d,  $J = 7.8$  Hz, 1H), 7.94 (d,  $J = 7.3$  Hz, 1H), 7.42 (m, 5H), 7.22 (t,  $J = 7.3$  Hz, 1H), 7.01 (s, 1H), 4.59 (m, 2H), 4.00 (m, 1H), 2.17 (m, 1H), 0.82 (d,  $J = 6.8$  Hz, 3H), 0.74 (d,  $J = 6.7$  Hz, 3H). Anal. (C<sub>26</sub>H<sub>22</sub>N<sub>3</sub>F<sub>3</sub>O<sub>5</sub>) C, H, N.

**General Method D. 2-[8-(Dimethoxyphosphoryl)-1-oxo-3-phenyl-1,2-dihydropyridol[3,4-*b*]indol-2-yl)-N-(3,3,3-trifluoro-2-hydroxy-1-isopropylpropyl)acetamide (37).** To a solution of **35** (2 g, 3 mmol) in ethanol (50 mL) was added 10% Pd/C (150 mg), and the mixture was shaken under a hydrogen atmosphere (50 psi) for 4 h. The mixture was filtered free of catalyst and the solvent removed to obtain the phenol as a white solid (1.6 g) sufficiently pure for further use. A portion of the phenol (1.21 g, 2.1 mmol) and triethylamine (0.62 mL, 4.4 mmol) were dissolved in dichloromethane (10 mL), and to this was added *N*-phenyltrifluoromethanesulfonimide (1.6 g, 4.4 mmol) followed by stirring for 12 h. The reaction mixture was poured into ether and washed with saturated aqueous sodium bicarbonate and H<sub>2</sub>O. The solution was dried (MgSO<sub>4</sub>), the solvent removed, and the resulting material chromatographed (gradient elution, 5% ethyl acetate/dichloromethane to 10% ethyl acetate/dichloromethane) to provide the triflate (1.2 g) as a white solid. The triflate (1.18 g, 1.8 mmol), dimethyl phosphite (0.5 mL, 5 mmol), *N*-methylmorpholine (0.8 mL, 6.6 mmol), and tetrakis(triphenylphosphine)-palladium(0) (0.19 g, 0.2 mmol) were combined in acetonitrile (5 mL), and the mixture was heated at 80 °C for 24 h. The reaction mixture was diluted with ethyl acetate and washed with 1 N HCl and H<sub>2</sub>O. The solution was dried and the solvent removed. The resulting material was chromatographed (gradient elution, ether to ethyl acetate) to provide the dimethyl phosphonate as a white solid (0.41 g). The phosphonate (0.41g, 0.61 mmol) was dissolved in a mixture of benzene (2 mL) and nitromethane (1 mL), and aluminum chloride (0.33 g, 2.5 mmol) was added. The mixture was stirred for 6 h, poured into ethyl acetate, and washed with 1 N HCl and H<sub>2</sub>O. The solution was dried (MgSO<sub>4</sub>), the solvent removed, and the product purified by chromatography (1% methanol/dichloromethane) to afford **37** (0.26 g, 21%) as a white solid: <sup>1</sup>H NMR (300 MHz, DMSO)  $\delta$  10.57 (s, 1H), 8.45 (d,  $J = 8.1$  Hz, 1H), 7.79 (m, 2H), 7.45 (m, 6H), 7.09 (s, 1H), 6.45 (br s, 1H), 4.60 (m, 2H), 4.11 (br s, 1H), 3.83 (t,  $J = 9.0$  Hz, 1H), 3.76 (s, 3H), 3.72 (s, 3H), 1.78 (m, 1H), 0.91 (d,  $J = 6.3$  Hz, 3H), 0.85 (d,  $J = 6.6$  Hz, 3H).

**2-[8-[(*tert*-Butyldimethylsilyloxy]-1-oxo-3-phenyl-1,2-dihydropyrido[3,4-*b*]indol-2-yl]-*N*-(3,3,3-trifluoro-2-hydroxy-1-isopropylpropyl)acetamide (36).** A solution of **35** (3.34 g, 5 mmol) in acetic acid (100 mL) was added to a mixture of palladium hydroxide (1.05 g) in acetic acid (100 mL) which had been prereduced with hydrogen. This solution was placed under a hydrogen atmosphere (40 psi) and heated at 80 °C overnight while shaking. The catalyst was filtered and the filter cake washed with THF. The filtrate and washings were combined, and the solvent was removed. The resulting material was triturated with dichloromethane to afford the desired debenzylated compound (1.18 g, 48%). A portion of this material (0.49 g, 1 mmol) was dissolved in DMF (2 mL), and to this was added imidazole (0.27 g, 4 mmol) and *tert*-butyldimethylsilyl chloride (0.21 g, 1.4 mmol) followed by stirring at room temperature for 48 h. The reaction mixture was diluted with ethyl acetate and washed with H<sub>2</sub>O and brine. The solution was dried (MgSO<sub>4</sub>), the solvent removed, and the product purified by chromatography (20% ethyl acetate/dichloromethane) to provide **36** (0.48 g, 80%) as a white foam: <sup>1</sup>H NMR (250 MHz, DMSO) δ 11.95 (s, 1H), 7.80 (d, *J* = 9.8 Hz, 1H), 7.65 (d, *J* = 8 Hz, 1H), 7.45 (m, 5H), 7.04 (t, *J* = 8 Hz, 1H), 6.90 (m, 3H), 6.48 (d, *J* = 7 Hz, 1H), 4.47 (m, 2H), 4.07 (m, 1H), 3.86 (t, *J* = 9 Hz, 1H), 1.79 (m, 1H), 1.01 (s, 9H), 0.92 (d, *J* = 6.8 Hz, 3H), 0.84 (d, *J* = 7.0 Hz, 3H), 0.32 (s, 6H); MS (CI) 602 (M + H).

**2-(8-Hydroxy-1-oxo-3-phenyl-1,2-dihydropyrido[3,4-*b*]indol-2-yl)-*N*-(3,3,3-trifluoro-1-isopropyl-2-oxopropyl)-acetamide (38).** A solution of **36** (0.48 g, 0.8 mmol) in THF (3 mL) was cooled to 0 °C, and to this was added tetra-*N*-butylammonium fluoride (1.0 mL, 1.0 mmol). The resulting solution was allowed to stir for 0.25 h. The reaction mixture was diluted with ethyl acetate and washed with saturated ammonium chloride, H<sub>2</sub>O, and brine. The solution was dried (MgSO<sub>4</sub>) and the solvent removed. The resulting material was triturated with dichloromethane to provide **38** (0.27 g, 70%) as a white solid: <sup>1</sup>H NMR (300 MHz, DMSO/*D*<sub>2</sub>O) δ 7.49 (d, *J* = 7.8 Hz, 1H), 7.42 (s, 5H), 7.04 (t, *J* = 7.5 Hz, 1H), 6.91 (s, 1H), 6.85 (d, *J* = 7.5 Hz, 1H), 4.57 (m, 2H), 4.02 (m, 1H), 2.17 (m, 1H), 0.82 (d, *J* = 6.5 Hz, 3H), 0.77 (d, *J* = 7.0 Hz, 3H). Anal. (C<sub>25</sub>H<sub>22</sub>F<sub>3</sub>N<sub>3</sub>O<sub>4</sub>·0.3H<sub>2</sub>O) C, H, N.

**Molecular Modeling.** Molecular mechanics computations were performed *in vacuo*, using the AESOP force field<sup>34</sup> and the in-house graphics program ENIGMA.<sup>35</sup> Only those residues within 12 Å of the active site region of the HLE-TOMI X-ray crystal structure were included in these computations. TOMI was removed, and HLE atoms were constrained to their position in the X-ray structure during energy minimization.

Molecular dynamics (MD)<sup>36</sup> simulations were performed using the program AMBER3.0a<sup>37</sup> and the united atom model. The starting geometry for HLE was taken from the X-ray molecular structure of the HLE-TOMI complex.<sup>24</sup> The non-covalently bound TOMI fragment was removed, as were the HLE-bound sugars, which are remote from the active site. Inhibitors were covalently attached via the trifluoromethyl carbonyl carbon to SER 195 as the oxyanion. The inhibitors were initially docked into the active site in a manner analogous to the arrangement observed for peptidic inhibitors in PPE. Carboxylic acids were modeled as their conjugate bases. Atomic partial charges were obtained for the β-carbolinone fragments of the inhibitors via electrostatic potential energy surface (EPS) fit to 6-31G\*\*/6-31G\* *ab initio* wave functions using the program SPARTAN 2.0.<sup>38</sup> United atom AMBER3.0a charges for valine were used for the P<sub>1</sub> portion of the inhibitor and the 3-position phenyl. Atom-centered charges employed in these simulations are reported in the supplementary material.

A 20 Å cap of TIP3P water with a weak restoring force<sup>37</sup> was placed over the active site of the enzyme-inhibitor complex. This resulted in the addition of approximately 450 water molecules to the computations. Initial structures were minimized for 250 cycles of steepest descent optimization prior to beginning dynamics. MD was initiated at 10 K and equilibrated to 298 K using an 8.0 Å cutoff radius. A time step of 0.001 ps was employed throughout the simulation, and data was collected every 0.1 ps. A pair list update was

performed every 0.02 ps. Simulations for each inhibitor or enzyme-inhibitor complex were performed over 50 ps, using the final 40 ps for analysis.

**Acknowledgment.** We thank Ms. Bobbie Scott for help in the preparation of this manuscript and Drs. Barrie Hesp, Andrew Shaw, Donald Wolanin, Philip Edwards, and Peter Warner for helpful discussions throughout the course of this work.

**Supplementary Material Available:** Atom-centered charges calculated for compounds **13a,d-f,h**, **19b**, and **34** (4 pages). Ordering information is given on any current masthead page.

## References

- (1) Travis, J.; Dumbin, A.; Potempa, J.; Watorek, W.; Kurdowska, A. Neutrophil Proteinases. *Ann. N.Y. Acad. Sci.* **1991**, *624*, 81–86.
- (2) Hornebeck, W.; Soleilhac, J. M.; Tixier, J. M.; Moczar, E.; Robert, L. Inhibition by Elastase Inhibitors of the Formyl Met Leu Phe-Induced Chemotaxis of Rat Polymorphonuclear Leukocytes. *Cell Biochem. Funct.* **1987**, *5*, 113–122.
- (3) Banda, M. J.; Rice, A. G.; Griffin, G. L.; Senior, R. M. α1-Proteinase Inhibitor Is a Neutrophil Chemoattractant after Proteolytic Inactivation by Macrophage Elastase. *J. Biol. Chem.* **1988**, *263*, 4481–4484.
- (4) Sandhaus, R. A. Elastase May Play A Central Role in Neutrophil Migration Through Connective Tissue. In *Pulmonary Emphysema and Proteolysis*; 1986; Taylor, J. C., Mittman, C., Eds.; Academic Press Inc.: New York, 1987; pp 227–234.
- (5) Sommerhoff, C. P.; Nadel, J. A.; Basbaum, C. B.; Caughey, G. H. Neutrophil Elastase and Cathepsin G Stimulate Secretion from Cultured Bovine Airway Gland Serous Cells. *J. Clin. Invest.* **1990**, *85*, 682–689.
- (6) Sommerhoff, C. P.; Krell, R. D.; Williams, J. C.; Gomes, B. C.; Strimpler, A. M.; Nadel, J. A. Inhibition of Human Neutrophil Elastase by ICI-200,355. *Eur. J. Pharmacol.* **1991**, *193*, 153–158.
- (7) Gadsek, J. E.; Fells, G. A.; Zimmerman, R. L.; Rennard, S. I.; Crystal, R. G. Antielastases of the human alveolar structures. Implications for the protease-antiprotease theory of emphysema. *J. Clin. Invest.* **1981**, *68*, 889–898.
- (8) Vogelmeier, C.; Hubbard, R. C.; Fells, G. A.; Schnebli, H. P.; Thompson, R. C.; Fritz, H.; Crystal, R. G. Anti-Neutrophil Elastase Defense of the Normal Human Respiratory Epithelial Surface Provided by the Secretory Leukoprotease Inhibitor. *J. Clin. Invest.* **1991**, *87*, 482–488.
- (9) Eriksson, S. The Potential Role of Elastase Inhibitors in Emphysema Treatment. *Eur. Respir. J.* **1991**, *4*, 1041–1043.
- (10) Nadel, J. Role of Mast Cell and Neutrophil Proteases in Airway Secretion. *Am. Rev. Respir. Dis.* **1991**, *144*, S48–S51.
- (11) Jackson, A. H.; Hill, S. L.; Afford, S. C.; Stockley, R. A. Sputum Soluble Phase Proteins and Elastase Activity in Patients with Cystic Fibrosis. *J. Respir. Dis.* **1984**, *65*, 114–124.
- (12) Tosi, M. F.; Zakem, H.; Berger, M. Neutrophil Elastase Cleaves C3bi on Opsonized Pseudomonas as well as CR1 on Neutrophils to Create a Functionally Important Opsonin Receptor Mismatch. *J. Clin. Invest.* **1990**, *86*, 300–308.
- (13) Edwards, P. D.; Bernstein, P. R. Synthetic Inhibitors of Elastase. *Med. Res. Rev.* **1994**, *14*, 127–194.
- (14) Bernstein, P. R.; Edwards, P. D.; Williams, J. C. Inhibitors of Human Leukocyte Elastase. *Prog. Med. Chem.* **1994**, *31*, 59–120.
- (15) (a) Peet, N. P.; Burkhart, J. P.; Angelastro, M. R.; Giroux, E. L.; Mehdi, S.; Bey, P.; Kolb, M.; Neises, B.; Schirlin, D. Synthesis of Peptidyl Fluoromethyl Ketones and Peptidyl α Keto Esters as Inhibitors of Porcine Pancreatic Elastase, Human Neutrophil Elastase, and Rat and Human Neutrophil Cathepsin G. *J. Med. Chem.* **1990**, *33*, 394–407. (b) Angelastro, M. R.; Bey, P.; Mehdi, S.; Janusz, M. J.; Peet, N. P. Janus Compounds: Dual Inhibitors of Proteinases. *Bioorg. Med. Chem. Lett.* **1993**, *3*, 525–530. (c) Doherty, J. B.; Shah, S. K.; Finke, P. E.; Dorn, C. P.; Hagmann, W. K.; Hale, J. J.; Kissinger, A. L.; Thompson, K. R.; Brause, K.; Chandler, G. O.; Knight, W. B.; Matcock, A. L.; Ashe, B. M.; Weston, H.; Gale, P.; Mumford, R. A.; Anderson, O. F.; Williams, H. R.; Nolan, T. E.; Frankfield, D. L.; Underwood, D.; Vyas, K. P.; Kari, P. H.; Dahlgren, M. E.; Mao, J.; Fletcher, D. S.; Dellea, P. S.; Hand, K. M.; Osinga, D. G.; Peterson, L. B.; Williams, D. T.; Metzger, J. M.; Bonney, R. J.; Humes, J. L.; Pacholok, S. P.; Hanlon, W. A.; Opas, E.; Stolk, J.; Davies, P. Chemical, biochemical, pharmacokinetic, and biological properties of L-680,833: A potent, orally active monocyclic β-lactam inhibitor of human polymorphonuclear leukocyte elastase. *Proc. Natl. Acad. Sci. U.S.A.* **1993**, *90*, 8727–8731.

- (16) Bergeson, S.; Schwartz, J. A.; Stein, M. M.; Wildonger, R. A.; Edwards, P. D.; Shaw, A.; Trainor, D. A.; Wolanin, D. J. U.S. Patent 4,910,190, 1990; *Chem. Abstr.* **1991**, *114*, 123085m.
- (17) Stein, M. M.; Wildonger, R. A.; Trainor, D. A.; Edwards, P. D.; Yee, Y. K.; Lewis, J. J.; Zottola, M. A.; Williams, J. C.; Strimpler, A. M. In Vitro and In Vivo Inhibition of Human Leukocyte Elastase (HLE) by Two Series of Electrophilic Carbonyl Containing Peptides. In *Peptides: Chemistry, Structure, and Biology (Proceedings of the Eleventh American Peptide Symposium)*; ESCOM Science: Lieden, The Netherlands, 1990; p 369.
- (18) (a) Williams, J. C.; Falcone, R. C.; Knee, C.; Stein, R. L.; Strimple, A. M.; Reaves, B.; Giles, R. E.; Krell, R. D. Biologic Characterization of ICI-200,880 and ICI-200,355, Novel Inhibitors of Human Neutrophil Elastase. *Am. Rev. Respir. Dis.* **1991**, *144*, 875-883. (b) Auger, W. R.; Moser, K. M.; Comito, R. M.; Kerr, K. M.; Bernardi, J. L.; Spragg, R. G. Efficacy of ICI 200,880, in the Prevention of Adult Respiratory Distress Syndrome (ARDS) in Patients undergoing Pulmonary Thromboendarterectomy, (abstract). *Am. Respir. Crit. Care Med.* **1994**, *149* (4), 1032. (c) Gottlieb, J. E.; Elmer, M.; Steiner, R.; Saller, L.; Minkwitz, M.; Glass, M. Efficacy of Intravenous ICI 200,880, A Neutrophil Elastase Inhibitor in the Treatment of Adult Respiratory Distress Syndrome (ARDS). *Chest* **1994**, in press.
- (19) (a) Brown, F. J.; Andisik, D. W.; Bernstein, P. B.; Bryant, C. B.; Ceccarelli, C.; Damewood, J. R., Jr.; Edwards, P. D.; Earley, R. A.; Feeney, S.; Green, R. C.; Gomes, B. C.; Kosmider, B. J.; Krell, R. D.; Shaw, A.; Steelman, G. B.; Thomas, R. M.; Vacek, E. P.; Veale, C. A.; Tuthill, P. A.; Warner, P.; Williams, J. C.; Wolanin, D. J.; Woolson, S. A. The Design of Orally Active, Nonpeptidic Inhibitors of Human Leukocyte Elastase. *J. Med. Chem.* **1994**, *37*, 1259-1261. (b) Warner, P.; Green, R. C.; Gomes, B. C.; Williams, J. C. Nonpeptidic Inhibitors of Human Leukocyte Elastase. 1. The Design and Synthesis of Pyridone-Containing Inhibitors. *J. Med. Chem.* **1994**, *37*, 3090-3099. (c) Damewood, J. R., Jr.; Edwards, P. D.; Feeney, S.; Gomes, B. C.; Steelman, G. B.; Tuthill, P. A.; Williams, J. C.; Warner, P.; Woolson, S. A.; Wolanin, D. J.; Veale, C. A. Nonpeptidic Inhibitors of Human Leukocyte Elastase. 2. Design, Synthesis, and In Vitro Activity of a Series of 3-Amino-6-arylpyridin-2-one-trifluoromethylketones. *J. Med. Chem.* **1994**, *37*, 3303-3312. (d) Bernstein, P. B.; Andisik, D.; Bradley, P. K.; Bryant, C. B.; Ceccarelli, C.; Damewood, J. R., Jr.; Earley, R.; Feeney, S.; Gomes, B. C.; Kosmider, B. J.; Steelman, G. B.; Thomas, R. M.; Vacek, E. P.; Veale, C. A.; Williams, J. C.; Wolanin, D. J.; Woolson, S. A. Nonpeptidic Inhibitors of Human Leukocyte Elastase. 3. Design, Synthesis, X-Ray Crystallographic Analysis, and Structure-Activity Relationships for a Series of Orally Active 3-Amino-6-phenylpyridin-2-ones. *J. Med. Chem.* **1994**, *37*, 3313-3326.
- (20) A related approach has also been reported; see: Skiles, J. W.; Sorcek, R.; Jacober, S.; Miao, C.; Mui, P. W.; McNeil, D.; Rosenthal, A. S. Elastase Inhibitors Containing Conformationally Restricted Lactams As P<sub>3</sub>-P<sub>2</sub> Dipeptide Replacements. *Bioorg. Med. Chem. Lett.* **1993**, *3*, 773-778.
- (21) Takahashi, S.; Radhakrishnan, R.; Rosenfield, R. E.; Meyer, E. F., Jr.; Trainor, D. A.; Stein, M. X-ray Diffraction Analysis of the Inhibition of Porcine Pancreatic Elastase by a Peptidyl Trifluoromethylketone. *J. Mol. Biol.* **1988**, *201*, 423-428.
- (22) Takahashi, L. H.; Radhakrishnan, R.; Rosenfield, R. E.; Meyer, E. F., Jr.; Trainor, D. A. Crystal Structure of the Covalent Complex Formed by a Peptidyl  $\alpha,\alpha$ -Difluoro- $\beta$ -keto Amide with Porcine Pancreatic Elastase at 1.78-Å Resolution. *J. Am. Chem. Soc.* **1989**, *111*, 3368-3374.
- (23) Edwards, P. D.; Meyer, E. F., Jr.; Vijayalakshmi, J.; Tuthill, P. A.; Andisik, D. A.; Gomes, B. C.; Strimpler, A. Design, Synthesis, and Kinetic Evaluation of a Unique Class of Elastase Inhibitors, the Peptidyl  $\alpha$ -Ketobenzoxazoles, and the X-ray Crystal Structure of the Covalent Complex between Porcine Pancreatic Elastase and Ac-Ala-Pro-Val-2-Benzoxazole. *J. Am. Chem. Soc.* **1992**, *114*, 1854-1863.
- (24) Bode, W.; Wei, A. Z.; Huber, R.; Meyer, E.; Travis, J.; Neumann, S. X-ray Crystal Structure of the Complex of Human Leukocyte Elastase (PMN Elastase) and the Third Domain of the Turkey Ovomuroid Inhibitor. *EMBO J.* **1986**, *5*, 2453-2458.
- (25) (a) Wei, A.-Z.; Mayr, I.; Bode, W. The Refined 2.3Å Crystal Structure of Human Leukocyte Elastase in a Complex with a Valine Chloromethylketone Inhibitor. *FEBS Lett.* **1988**, *234*, 367-373. (b) Navia, M. A.; McKeever, B. M.; Springer, J. P.; Lin, T. Y.; Williams, H. R.; Fluder, E. M.; Dorn, C. D.; Hoogsteen, K. Structure of Human Neutrophil Elastase in Complex with a Peptide Chloromethyl Ketone Inhibitor at 1.84Å Resolution. *Proc. Natl. Acad. Sci. U.S.A.* **1989**, *86*, 7-11.
- (26) Bode, W.; Meyer, E., Jr.; Powers, J. C. Human Leukocyte and Porcine Pancreatic Elastase: X-ray Crystal Structures, Mechanism, Substrate Specificity, and Mechanism-Based Inhibitors. *Biochemistry* **1989**, *28*, 1951-1963.
- (27) Abramovitch, R. A.; Shapiro, D. Tryptamines, Carbolines, and Related Compounds. *J. Chem. Soc.* **1956**, 4589-4592.
- (28) Bernstein, P. R.; Shaw, A.; Thomas, R. M.; Warner, P.; Wolanin, D. J. European Patent Appl. No. 509,769 A2, 1992.
- (29) Murakami, Y.; Tani, M.; Ariyasu, T.; Nishiyama, C.; Watanabe, T.; Yokoyama, Y. The Friedel-Crafts Acylation of Ethyl Pyrrole-2-Carboxylate. *Heterocycles* **1988**, *27* (8), 1855-1860.
- (30) Edwards, P. D.; Lewis, J. J.; Perkins, C. W.; Trainor, D. A.; Wildonger, R. A. European Patent Appl., Publication No. 0 291 234 A2, 1988.
- (31) Williams, J. C.; Stein, R. L.; Strimpler, A. M.; Reaves, B.; Krell, R. D. *Exp. Lung Res.* **1991**, *17*, 725-741.
- (32) This had previously been observed in the 6-phenylpyridone series where addition of a phenyl group to the 6-position of the pyridone ring resulted in a 5000-fold increase in affinity for bovine pancreatic chymotrypsin.
- (33) Shaw, S. K.; Dorn, C. P.; Finke, P. E.; Hale, J. J.; Hagmann, W. K.; Brause, K. A.; Chandler, G. O.; Kissinger, A. L.; Ashe, B. M.; Weston, H.; Knight, W. B.; Maycock, A. L.; Dellea, P. S.; Fletcher, D. S.; Hand, K. M.; Mumford, R. A.; Underwood, D. J.; Doherty, J. B. Orally Active  $\beta$ -Lactam Inhibitors of Human Leukocyte Elastase-1. Activity of 3,3-Diethyl-2-azetidiones. *J. Med. Chem.* **1992**, *35*, 3745.
- (34) AESOP is an in-house molecular mechanics program (Masek, B.; Zeneca, Inc., 1800 Concord Pike, Wilmington, DE 19897) derived from BIGSTRN-3 (QCPE 514) (Nachbar, R., Jr.; Mislow, K. *QCPE Bull.* **1986**, *6*, 96).
- (35) ENIGMA is an in-house molecular graphics program (Zeneca, Inc., 1800 Concord Pike, Wilmington, DE 19897).
- (36) For reviews of the molecular dynamics method, see: McCammon, J. A.; Harvey, S. C. *Dynamics of Proteins and Nucleic Acids*; Cambridge University Press: New York, 1987. Brooks, C. L., III; Karplus, M.; Pettitt, B. M. *Proteins: A Theoretical Perspective of Dynamics, Structure and Thermodynamics*; John Wiley & Sons: New York, 1988. van Gunsteren, W. F.; Weiner, P. K. *Computer Simulation of Biomolecular Systems. Theoretical and Experimental Applications*; Escom: Leiden, 1989.
- (37) Singh, U. C.; Weiner, P.; Caldwell, J. C.; Kollman, P. A. AMBER 3.0 Revision A.; University of California: San Francisco, 1989.
- (38) SPARTAN 2.0; Wavefunction, Inc., 18401 Von Karman, Suite 210, Irvine, CA 92715.

JM9404996